Electrochemical synthesis of hydrogen peroxide from water and oxygen

Samuel C. Perry[1]*, Dhananjai Pangotra[3,4], Luciana Vieira[3], Lénárd-Istvan Csepei[3], Volker Sieber[3,4], Carlos Ponce de León[1,2], Ling Wang[1,2], Frank C. Walsh[1,2]

[1] Electrochemical Engineering Laboratory, Faculty of Engineering and the Environment,

University of Southampton, Highfield, Southampton, SO17 1BJ, UK

[2] National Centre for Advanced Tribology at Southampton (nCATS), Faculty of Engineering and the Environment, University of Southampton, Southampton SO17 1BJ, UK

[3] Fraunhofer Institute for Interfacial Engineering and Biotechnology IGB, 94315 Straubing, Germany

[4] Technical University of Munich, Straubing Campus for Biotechnology and Sustainability, Schulgasse 16, 94315 Straubing, Germany

*email: S.C.Perry@soton.ac.uk

Abstract

H_2O_2 is important in large-scale industrial processes and smaller on-site activities. The present industrial route to H_2O_2 involves hydrogenation of an anthraquinone and O_2 oxidation of the resulting dihydroanthraquinone - a costly method and one that is impractical for routine on-site use. Electrosynthesis of H_2O_2 is cost-effective and applicable on both large and small scales. This Review describes methods to design and assess electrode materials for H_2O_2 electrosynthesis. H_2O_2 can be prepared by oxidizing H_2O at efficient anodic catalysts such as those based on $BiVO_4$. Alternatively, H_2O_2 forms by partially reducing O_2 at cathodes featuring either noble metal alloys or doped carbon. In addition to the catalyst materials used, one must also consider the form and geometry of the electrodes and the type of reactor in order to strike a balance between properties such as mass transport and electroactive area, both of which substantially affect both the selectivity and rate of reaction. Research into catalyst materials and reactor designs is arguably quite mature, such that the future of H_2O_2 electrosynthesis will instead depend on the design of complete and efficient electrosynthesis systems, in which the complementary properties of the catalysts and the reactor lead to optimal selectivity and overall yield.

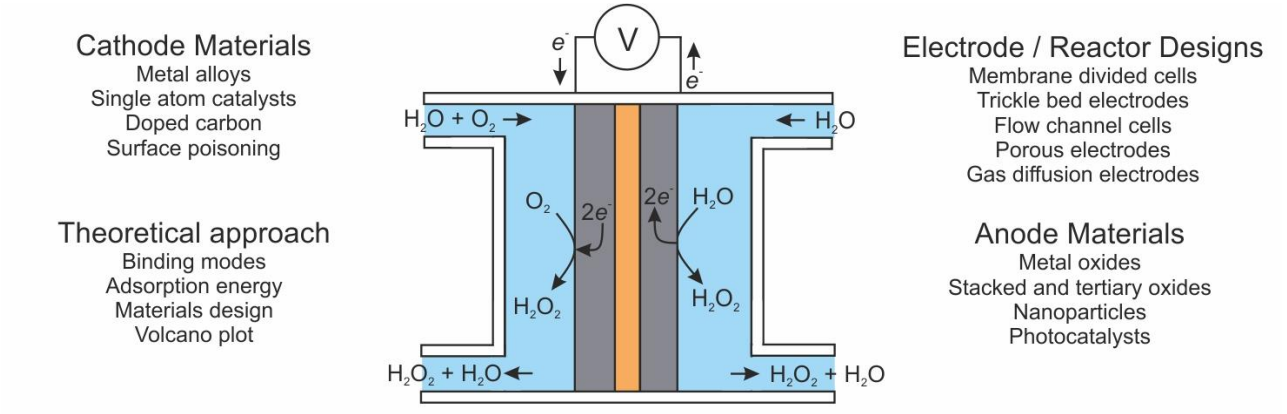

Introduction

H_2O_2 is a strong oxidant with many uses both in a domestic setting as well as in industrial bleaching,[1] waste water treatment,[2-5] chemical synthesis[6-10] and fuel cell technologies.[11, 12] These applications see H_2O_2 produced on a scale of approximately 2.2 million tonnes per year.[1] a value that can be expected to increase given that H_2O_2 is a more environmentally friendly oxidant than Cl-based oxidants such as HOCl. At present, 95% of H_2O_2 is produced through the anthraquinone process,[13] which begins with the hydrogenation of a 2-alkyl-9,10-anthraquinone in an organic solvent over a Pd catalyst.[14] In solution, the resulting dihydroanthraquinone then undergoes rapid oxidation by O_2 to give H_2O_2 and regenerate the

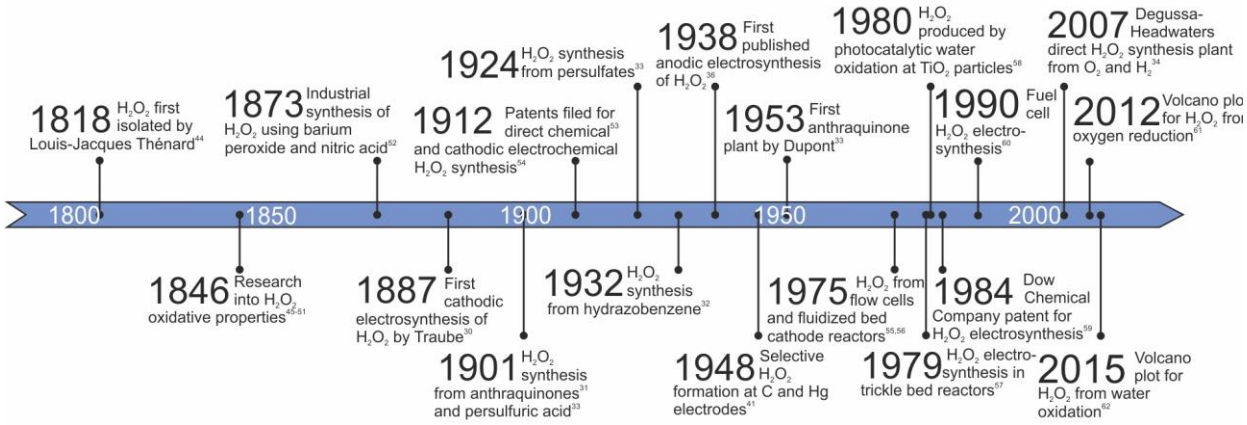

Figure 1 | **The major developments in the chemical and electrochemical synthesis of H_2O_2.**

anthraquinone. The H_2O_2 is removed by solvent extraction, leaving anthraquinone in the organic phase to be recycled.[15] This batch process typically affords large volumes of highly concentrated aqueous H_2O_2, which poses safety risks in terms of stability, storage and transport.[16] Aside from the specialty aerospace industry,[17] few sectors require H_2O_2 in a concentrated form, such that the risks associated with its preparation are unjustified. Moreover, the regeneration of the anthraquinone is not 100% efficient, but participates in a number of side reactions. The dihydroanthraquinone can be further hydrogenated to give more saturated products including tetra- or octahydroanthraquinone, and carbonyl groups can undergo hydrogenolytic cleavage to give 2-ethylanthrone, which also participates in further reactions to give 2-ethyleneanthracene.[18] Highly oxidizing conditions can also oxidize the dihydroanthraquinone to give the corresponding epoxide.[19] The anthraquinone therefore requires constant replenishment to maintain a satisfactory rate of H_2O_2 production.[13] With these shortcomings in mind, there is a push to develop a more energy-efficient and resource-efficient route that is amenable to on-site production of H_2O_2 in dilute working concentrations.[20]

A popular alternative to the anthraquinone process is the direct synthesis of H_2O_2 from H_2 and O_2. This partial hydrogenation is normally performed at low temperatures by passing gas mixtures over a noble metal catalyst such as Pd.[21] These catalysts also mediate competing side reactions, including the combustion of H_2 to H_2O, the hydrogenation of H_2O_2 to H_2O and the decomposition of H_2O_2 to H_2O and $½O_2$.[22] Perhaps the most substantial barrier to the development of this synthetic route is the need to work with mixtures of H_2 and O_2, which are explosive over a wide composition range (4–94 mol%H_2).[23] This danger means that the reactants are diluted with a relatively inert carrier gas such as CO_2. However, this dilution and the inherent thermodynamic favourability of the side reactions reduce the practically achievable overall yields of the direct synthesis.

H_2O_2 is produced in nature through a range of enzymatic processes. Oxidase enzymes such as glucose oxidase,[24] D-amino acid oxidase[25] and cholesterol oxidase,[26] produce H_2O_2 when presented with their native substrates. The limited turnover frequencies of these systems has limited their utility for H_2O_2 synthesis, although these enzymes are used in biosensing applications, in which quantifying an enzyme substrate can be performed indirectly by measuring how much H_2O_2 it affords.[27, 28] Other possible applications include food sanitation, in which H_2O_2 generated by glucose oxidase could be used to protect food against microorganisms.[29]

Electrochemistry offers an economical and environmentally friendly route to H_2O_2 either from H_2O or O_2. Indeed, H_2O_2 can be produced at either an anode or cathode surface and can accumulate in useful concentrations over continued electrolysis. The first published example of H_2O_2 electrosynthesis came from Traube in 1887, who produced H_2O_2 from O_2 at a Hg-Au electrode.[30] At the time, this method was less efficient than chemical syntheses of H_2O_2, which included O_2 oxidation of hydrazobenzenes,[31, 32] hydrolysis of persulfates[33] (which, in turn, are prepared by electrolysis of bisulfates in H_2SO_4) or direct synthesis.[34] The first H_2O_2 synthesis plant was built by Dupont in 1953 and used the anthraquinone process.[33] Although chemical syntheses have dominated industrial H_2O_2 production, since Traube's report electrosyntheses have appeared continually in the literature, including methods with improved yields[35] and anodic electrosynthesis.[36-38] Indeed, understanding the kinetics of the redox reactions involving O_2, H_2O_2 and H_2O[39-41] enabled rational designs of electrodes

with high current densities[35, 42] and/or selectivities[41, 43] have resulted in the development of increasingly efficient catalysts. The major developments in this field are summarised in Figure 1.

Nowadays, laboratory H_2O_2 electrosyntheses are typically carried out in reactor volumes of hundreds of milliliters. Scaling these experiments up to industrially relevant volumes whilst preserving the same principles is likely possible given the number of reports that describe pilot plants operating on an intermediate scale.[63-65] Alternatively, it is possible to produce H_2O_2 in situ for immediate consumption in oxidation reactions, such as the epoxidation of alkenes,[66, 67] or the synthesis of peracetic acid[68] or benzamide.[69] Such in situ methods have distinct advantages over other synthetic routes, and in the case of epoxidation, for example, the local concentrations of H_2O_2 at the electrode are high enough to drive the reaction without the need for H_2O_2 to be present in high concentrations throughout the reactor.

As we mentioned above, the development of H_2O_2 electrosynthesis catalysts is complicated because many common electrode materials favour competing reactions. Thus, the $4e^-$ reduction of O_2 (the oxygen reduction reaction, ORR) or $4e^-$ oxidation of $2H_2O$ (the oxygen evolution reaction, OER) is undesirable because we require $2e^-$ reduction of O_2 or $2e^-$ oxidation of $2H_2O$ to get H_2O_2. The electrosynthesis of H_2O_2 is a relatively unusual process because it involves reversible redox reactions of starting materials, intermediates and products. This makes it more challenging than processes that focus on one reaction to give a stable product.

A lot of research on electrocatalytic O_2 reduction and H_2O oxidation is motivated by renewable energy applications, for which complete $4e^-$ reduction of O_2 is desirable because it affords the maximum power output. Thus, electrodes that produce H_2O_2 are considered flawed for fuel cell applications but are desirable in that they afford an industrially useful chemical in a green synthesis, particularly in the context of paired electrochemical processes. Most experimental research focuses on catalyst development, but the combination of experiment and theory enables more rational studies geared towards H_2O_2 formation whilst suppressing its redox reactions that afford either H_2O or O_2. A number of efficient electrosynthesis cell designs already exist for other reactions, but the key requirement particular to our reactions of interest is the separation of anode and cathode to attenuate the decomposition of H_2O_2 after its electrosynthesis.

This Review is an overview of the recently disclosed electrocatalysts that are selective for H_2O_2 as the end product, as well as the reactor designs that can best exploit these materials to generate the maximum possible H_2O_2 output. We describe the key advances required in H_2O_2 electrosynthesis to see it progress from laboratory-scale operations to larger industrial-scale applications.

Thermodynamics of H_2O_2 production

The $2e^-$ oxidation of $2H_2O$ can proceed electrochemically to give H_2O_2.[70] All potentials are given verus the standard hydrogen electrode (SHE)

$$2H_2O \rightleftharpoons H_2O_2 + 2H^+ + 2e^- \quad E^0 = 1.760\ \text{V} \qquad (1)$$

Complications arise because the desired product H_2O_2 can undergo further oxidation:

$$H_2O_2 \rightleftharpoons O_2 + 2H^+ + 2e^- \quad E^0 = 0.670\ \text{V} \qquad (2)$$

The standard potential for the formation of H_2O_2 is more positive than that for the further oxidation of H_2O_2 to O_2, so any H_2O_2 that forms may be easily oxidized, lowering the yield. Many electrochemical cells are optimized for the OER, either via H_2O_2 or by direct $4e^-$ oxidation of $2H_2O$:

$$2H_2O \rightleftharpoons O_2 + 4H^+ + 4e^- \quad E^0 = 1.229\ \text{V} \qquad (3)$$

Thermodynamics also complicate the selective cathodic electrosynthesis of H_2O_2 because the reduction of O_2 has a more negative standard potential than does H_2O_2, meaning that further reduction of H_2O_2 is favoured, lowering the yield of H_2O_2. Another deleterious reaction is the spontaneous disproportionation of H_2O_2 to give H_2O and $½O_2$.[71]

$$2H_2O_2 \rightleftharpoons O_2 + 2H_2O \qquad (4)$$

In addition to the $2e^-$ reductions and oxidations we have described, a number of $1e^-$ redox reactions involving oxygenic species have been proposed to be operative:[72-74]

$$O_2 + e^- \rightarrow O_2^{\bullet -} \quad E^0 = 0.330\ \text{V} \qquad (5a)$$

$$O_2 + 3H^+ + 3e^- \rightarrow HO^\bullet + H_2O \quad E^0 = 0.803\ \text{V} \qquad (5b)$$

$$H_2O_2 + e^- \rightarrow HO^\bullet + OH^- \quad E^0 = 0.104\ \text{V} \qquad (5c)$$

The oxygenic radicals can contribute to the formation of H_2O_2, either by further electron transfers or through solution reactions following the superoxide dismutation:[75]

$$O_2^{\bullet-} + H^+ \rightleftharpoons HO_2^{\bullet} \quad (6a)$$

$$O_2^{\bullet-} + HO_2^{\bullet} \rightarrow HO_2^- + O_2 \quad (6b)$$

$$HO_2^{\bullet} + e^- \rightleftharpoons HO_2^- \qquad E^0 = -0.744\ V \quad (6c)$$

$$HO_2^- + H^+ \rightleftharpoons H_2O_2 \quad (6d)$$

H_2O_2 may also undergo homolysis to $HO^{\bullet}$ radicals,[76] which are strongly oxidizing.[72]

$$H_2O_2 \rightarrow 2OH^{\bullet} \quad (7a)$$

$$HO^{\bullet} + H^+ + e^- \rightleftharpoons H_2O \qquad E^0 = 2.330\ V \quad (7b)$$

Systems for the preferential formation of H_2O_2 should favour initial redox to give H_2O_2, whilst also allowing for rapid diffusion of H_2O_2 away from the electrode before it can undergo (deleterious) further oxidation or reduction.

Energy and bonding

We have described the reversible redox reactions between H_2O, H_2O_2 and O_2, but we stress that the interplay of these reactions is highly surface dependent. For O_2 reduction, the rate determining step is as yet unknown even at relatively simple materials like Pt.[77] Experimentally, Tafel analysis indicates that it is the first electron transfer that is rate determining.[78] This does not reveal whether the electron transfer is coupled to O_2 protonation or dissociative adsorption,[79] although it has been proposed that the electron transfer precedes dissociation because the activation energy for the dissociation of adsorbed OOH is much smaller than for O_2.[80] Computational studies have also proposed other rate determining steps such as breaking the O–O bond[81] or the reduction of PtO[82] due to the large calculated activation energies for these reaction steps. This presents the possibility of different rate determining steps for different crystal faces, due to their vaied adsorption energies towards ORR intermediates.[83] A consistent observation is that interaction between O_2 and the electrode surface is important in predicting the efficiency of a catalyst for H_2O_2 production, hence the sizeable impact of crystal face and pH on the reaction rate.[84] Most metal surfaces have a strong affinity for O_2, such that the (electro)adsorption of O_2 precedes e^- transfer.[79] One exception to this is Au, which first performs $1e^-$ reduction on O_2 through an outer-sphere mechanism.[85] Regardless of which process occurs first, if we consider the complete $4e^-$ reduction at a metal M there will be multiple oxygenic intermediates, each of which will have different M–O interactions.

There are a number of different ways in which O_2 can adsorb onto a metal surface. O_2 can bind side-on to a single metal centre in an $M(\eta^2\text{-}O_2)$ arrangement referred to as the Griffith model.[86] This model, by analogy with the Dewar–Chatt–Duncanson model for olefin binding, involves donation from the O_2 2π orbital to the empty M-centred d_{z2} orbital, with synergistic backbonding from partially filled d_{xy} or d_{yz} M-centred orbitals into the $2\pi^*$ orbital of O_2.[87] Alternatively, O_2 can bridge two metal sites in a $M(\mu,\eta^2\text{-}O_2)M$ motif called the bridge model .[88] The strong σ interactions lead to strong π backbonding that weakens the O–O bond and promotes dissociative adsorption. In both these binding modes both O atoms are bound to a metal site, which hinders any H_2O_2 intermediates from leaving the electrode before they can undergo reduction as part of the complete $4e^-$ ORR.[80, 89] In contrast, the $M(\eta^1\text{-}O_2)$ binding mode, known as the Pauling model features donation from an O-centred sp^2 hybrid orbital into the M-centered d_{z2} orbital. This alone cannot lead to O_2 dissociation and thus favours $2e^-$ redox with H_2O_2 as the end product.[87]

In addition to the orientation of binding, the strength of the interactions also influences the products of the redox reactions. Stronger M–O bonds arise when M donates substantial electron density to the adsorbed O_2 molecule. In such a case, the activation energies of the O-centred reductions that sequentially convert O_2 to $O_2^{\bullet-}$, H_2O_2 and then $OH^{\bullet}$ are low. However, then the activation enthalpy associated with the final step — reduction of adsorbed $OH^{\bullet}$ — becomes high[89] and the electrode surface can become poisoned by the highly stable M–OH groups. Thus, in this strong bonding case, catalytic turnover can be slow and will favour H_2O instead of H_2O_2 as the final product.

A number of studies have described tuning the binding energy between oxygenic species and metal surfaces (ΔG_O) in order to rationally design catalysts to be selective for the ORR, OER or H_2O_2 synthesis.[61, 90-94] As we have seen for the ORR, the highest catalytic activity occurs when ΔG_O is an intermediate value — binding is strong enough to favour the initial adsorption, but weak enough to release $OH^{\bullet}$ to prevent surface poisoning and complete the catalytic cycle. It is often thought that the optimal ORR catalyst can be arrived at by finding the optimal ΔG_O value, which is sensitive to the identity of metal[90, 94]/alloy[91-93] and facet.[61, 84] This approach has led to the design of new ORR catalysts based on a number of Pt and Pd alloys,[95-104] and OER perovskite catalysts such as $Ba_{0.5}Sr_{0.5}Co_{0.8}Fe_{0.2}O_{3-\delta}$.[105, 106]

When targeting the selective synthesis of H_2O_2 from either O_2 or H_2O we want a cathode or anode that binds H_2O_2 weakly, such that the product can

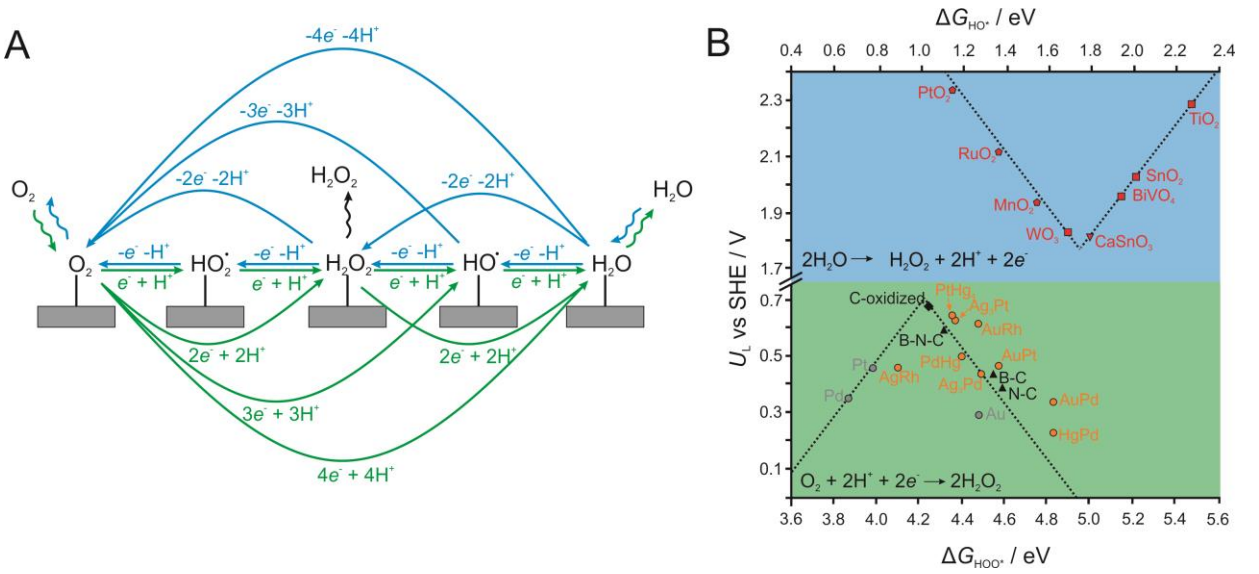

Figure 2. | **Interactions between intermediates and the catalyst surface strongly affect rates of H_2O_2 electrosynthesis. a |** The possible reduction pathways from O_2 to H_2O (green) and oxidation pathways from H_2O to O_2 (blue). The grey arrows denote mass transport of species between the bulk solution and the catalyst. Stoichiometric H_2O is omitted for clarity. **b** | A plot of theoretical limiting potential (U_L) against Gibbs free energies of binding *OOH (ΔG_{HOO*}) and *OH (ΔG_{HO*}) for H_2O_2 electrosynthesis. U_L is the least positive (anodic) or negative (cathodic) potential at which both electron transfers are downhill in free energy (the potential where the free energy surface becomes completely exergonic). The green region represents O_2 reduction and the blue region H_2O oxidation. Catalysts are categorized as pure metals (grey), metal alloys (yellow), carbon-based materials (black) and metal oxides (red). The dashed lines represent the theoretical Sabatier volcanoes,[61] the peaks of which corresponds to parameters of theoretical optimum catalysts. Part **b** was drawn from data in REFs 129 (■), 109 (●), 131 (▲) 108 (◆) 132 (▼) and 62 (⬟). For many materials, the exact U_L depends on the surface site (step, edge, basal plane etc.) so the most favourable U_L is shown in each case.

dissociate from the surface instead of undergoing further $2e^-$ reduction or oxidation as part of a complete ORR or OER. The binding energies of the superoxo intermediate (ΔG_{HOO*} for M + OOH → MOOH)[107, 108] and of the hydroxo intermediate (ΔG_{HO*} for M + OH → MOH)[61, 109-111] have been identified as useful descriptors for catalysts to favour H_2O_2 formation from O_2 or H_2O, respectively (FIG. 2). Alloying Hg with metals commonly used for the ORR has a large effect on ΔG_{HOO*}, giving a volcano-type relationship between ΔG_{HOO*} and the resulting activity for H_2O_2 formation, with Pd-Hg alloys outperforming other sampled alloys.[107] This example also allows us to illustrate that ΔG_{HOO*} scales linearly with ΔG_{HO*}, such that the values can be used interchangeably.[109] The scaling relationship between these descriptors can be detrimental because it can be difficult to change one without changing the other.[112] For the ORR, catalyst turnover rate could be increased by reducing ΔG_{HO*} to prevent surface poisoning by the hydroxo intermediate, but this would need to be done without reducing ΔG_{HOO*}, otherwise the superoxo intermediate could be released before the ORR reaches completion. Fundamentally, the difference between the free energies of HO* and HOO* should be 2.46 eV (twice the equilibrium potential for the ORR) but the scaling constrains the difference to ≈ 3.3 eV, which gives limits the maximum efficiency of any catalyst towards the ORR.[113] Countering the scaling between ΔG_{HOO*} and ΔG_{HO*} has already been the subject of works to develop new ORR catalysts, by modifying catalyst covalence[114] or using a tandem bi-functional catalyst where one component is optimised towards ΔG_{HO*} and the other towards ΔG_{HOO*}.[115]

We have mentioned the large body of ORR and OER research, and noted a recent push to also design catalysts for the $2e^-$ reduction of O_2 to H_2O_2. There has also been attention paid to the rational design of catalysts for the $2e^-$ oxidation of $2H_2O$ to H_2O_2. As with the ORR, the bulk of the OER literature has focused on the complete $4e^-$ pathway, in this case giving O_2.[116-128] Catalysts now also exist for the selective anodic synthesis of H_2O_2. These catalysts are often transition metal oxides, and include materials that are free of noble metals. Density functional theory (DFT) calculations on the adsorption of OER reaction intermediates revealed that ΔG_{HO*} and ΔG_{O*} are useful descriptors to predict the suitability of a material for anodic H_2O_2 electrosynthesis.[62, 129, 130]

Materials

The first published example of H_2O_2 electrosynthesis involved using a Hg-Au electrode to reduce O_2 and afford only a few milligrams of H_2O_2.[30] A major advancement came with instead using highly porous activated carbon electrodes, which greatly increased the electrode surface area to increase the overall rate of production.[35] These porous carbon cathodes formed the substrate for subsequent electrocatalysts for many years.[133, 134] As the field advanced, the electrode materials became more complex, moving towards doped

Table 1 | **Electrode materials for the electrosynthesis of H_2O_2.** The methods and apparatus used to assess these methods include a gas diffusion electrode (GDE), rotating ring disc electrode (RRDE), chronoamperometry (CA), linear sweep voltammetry (LSV) and photovoltaic cell (PVC). Where multiple compositions of doped or alloyed materials were studied, the best recorded value is shown.

[a] Value calculated assuming efficiency = $(2 - n/2) \times 100\%$, where n is the number of electrons.[148] [b] pH was not explicitly reported but has been approximated here based on the electrolyte used. [c] Demonstrative potentials and current densities were read off steady state voltammograms. [d] Demonstrative potentials and current densities determined from a Koutecký–Levich plot.

Material	Faradaic Efficiency / %	*n*	Anodic / Cathodic	Method	Solution	pH	*E vs.* RHE / V	*j* / mA cm^{-2}	Ref
Carbon									
Carbon nanotubes	90[a]	1.8	Cathodic	RRDE	0.1 M KOH	13[b]	-	-	135
Mesoporous carbon	95	2.1[a]	Cathodic	GDE	0.5 M NaOH	13.7[b]	0.43	-150	136
Doped carbon									
N-C (mesoporous)	95	2.1	Cathodic	RRDE	0.1 M H_2SO_4	0.3	0.10	-1.25[c]	137
Boron doped diamond	53	2.9[a]	Cathodic	CA	0.5 M H_2SO_4	1[b]	-1.74[c]	-	138
Carbon macrocycles									
Co(II) phthalocyanine	81.5	2.3	Cathodic	GDE	0.1 M K_2SO_4	2[b]	0.23	-0.02[c]	139
Fe(II) phthalocyanine	78.2	2.4	Cathodic	GDE	0.1 M K_2SO_4	2[b]	-0.18	-0.01[c]	140
Single atom catalyst									
Pt/S doped carbon	96	2.1	Cathodic	RRDE	0.1 M $HClO_4$	1.3[b]	0.1[c]	-0.05[c]	141
Metal Alloy Nanoparticles / Carbon									
$Au_{0.92}Pd_{0.08}$/carbon black	95	2.1[a]	Cathodic	RRDE	0.1 M $HClO_4$	1[b]	0.0	-0.8[c]	142
Sn_6Ni/carbon black	88	2.2	Cathodic	RRDE	1 M NaOH	14[b]	0.7[d]	-0.34[d]	143
Metal Oxide Nanoparticles / Carbon									
CeO_2/carbon black	95	2.1[a]	Cathodic	RRDE	1 M NaOH	14[b]	0.84	-0.15[c]	144
WO_3/Vulcan carbon	84	2.3	Cathodic	GDE	0.1 M K_2SO_4	0.3[b]	-1.08	-	145
Metal oxides									
$BiVO_4$	95	2.1[a]	Anodic	LSV	1 M $NaHCO_3$	8.3	2.8[c]	15[c]	129
$CaSnO_3$	76	2.5[a]	Anodic	CA	2 M $KHCO_3$	8.3	3.2	34[c]	132
Mixed metal oxides									
$BiVO_4$/WO_3/Al_2O_3	80	2.4[a]	Photo-oxidative	PVC	2 M $KHCO_3$	7.9	-	1	146
IrO_2/Ta_2O_5	79.3	2.4[a]	Cathodic	CA	0.1 M Na_2SO_4	7	-	0.001	147

carbons, noble metal alloys and metals oxides. The development of computational methods to predict the activity of materials towards H_2O_2 electrosynthesis drove further improvements in catalyst materials, as experimental papers worked towards the peak of the Sabatier volcano plot predicted from DFT calculations.[107, 129]

For all materials, there is an inverse relationship between the current density and the selectivity towards H_2O_2. A number of materials offer excellent selectivity towards H_2O_2 when working at small overpotentials and low total rates but then become poorly selective when working at higher total rates. Even the simplest of materials can have excellent selectivity for H_2O_2 formation provided the reaction is driven at low overpotentials. However, catalysts for real applications will need to maintain their selectivity even when working at current densities in the order of hundreds of milliamperes per square centimetre. When comparing materials, it is vital to consider the overpotential at which a given selectivity for H_2O_2 is reported, and one should determine the selectivity of a material over a range of overpotentials. Some of the leading materials for H_2O_2 electrosynthesis are given in Table 1, along with the conditions used to measure their selectivities. We now describe some of these materials and highlight mechanistic origins of their high selectivities.

Pure metals

It has become common to analyze materials for their H_2O_2 electrosynthesis activity because applications in fuel cells demand ORR catalysts that produce a minimum of H_2O_2 even when working at low overpotentials. In practice, any H_2O_2 that forms can be detected either at the ring of a rotating ring–disc electrode (RRDE),[149-153] by scanning electrochemical microscopy (SECM)[154-158] or inferred from a decrease in the apparent number of electrons transferred (n) per O_2 substrate from the ideal ORR value of 4.[91, 159-164] Thus, ORR (or OER) catalysts that effect incomplete reduction or oxidation are less useful for fuel cells but may be of great use for H_2O_2 electrosynthesis, in which failed ORR or OER catalysts may be suitable for H_2O_2 production. The selectivity towards H_2O_2 formation at pure metals depends strongly on the applied potential. In the case of the ORR, SECM shows that Hg, Au, Ag, Cu, Pt and Pd all generate some H_2O_2 at low overpotentials. However, only Hg maintains high selectivity for H_2O_2 at all potentials studied (FIG. 3).[154]

Although it is encouraging that all materials can produce H_2O_2 when poised at a certain overpotential, the requirement of a low overpotential can result in inherently low current densities. Alternatively, a given material can be tuned to favour H_2O_2 production by increasing the rate of mass transport to/from the electrode surface, in which case H_2O_2 diffuses rapidly from the electrode before it can undergo further reactions. Increasing the rate of mass transport has been achieved using microelectrodes[159, 160] rotating disc electrodes,[159, 163] nanoparticles[164, 165] and flow cells,[166] by varying physical parameters such as electrode radius, catalyst loading, particle

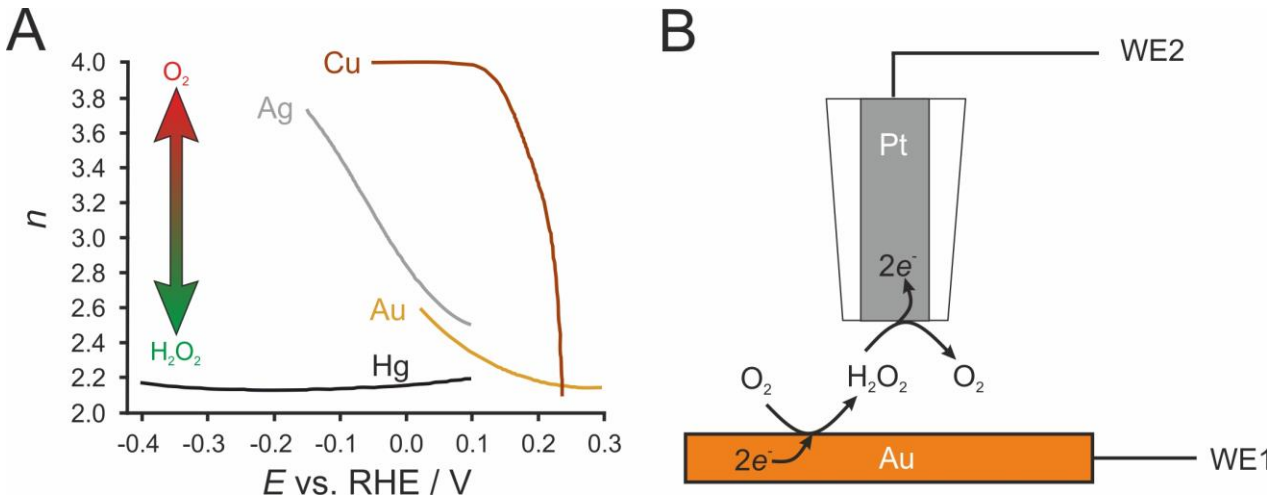

Figure 3. | **O_2 reduction to H_2O_2 at metal electrodes. a |** The number of electrons transferred (n) to O_2 at Hg, Au, Ag and Cu as a function of applied potential, with data recorded in H_2SO_4 (0.5 M aqueous) electrolyte. **b** | The electrode setup used to generate H_2O_2 and quantify its formation. Working electrode 1 (WE1) is 2 mm in diameter and is biased at potential E to generate H_2O_2. Located 50 μm away from WE1 is working electrode 2 (WE2), a 25 μm diameter microelectrode biased sufficiently positively to oxidize H_2O_2, thereby detecting it in the form of an anodic current. The ratio of currents at WE1 and WE2 are used to calculate n. Part **a** was drawn from data in REF 154.

shape/size, rotation rate or flow rate. The effect of using small nanoparticles is not just a physical one — smaller particles favour the end-on O_2 binding mode that can selectively afford H_2O_2. Indeed, the size of Pt clusters on the inert support indium tin oxide (ITO) is inversely proportional to the selectivity with which they electrogenerate H_2O_2 from O_2.[167] Although the increase in H_2O_2 production under conditions of high mass transport is substantial, the materials do not give 100% H_2O_2 selectivity (n = 2), so most works focus on more practical solutions such as alloys and composites.

Metal alloys

Some of the most successful materials for H_2O_2 electrosynthesis by oxygen reduction are based on metal alloys, such as Pd-Au,[16, 168] Pt-Pd,[169] W-Au,[170] or Pt-Hg.[107, 109] As we described above, these catalysts are often designed through calculations that predict the optimal strength of O_2 adsorption.[90, 129] Computational studies have correctly predicted the performance of evenly dispersed[107, 109] and core-shell alloy[96, 170, 171] catalysts. The two metals that are alloyed do not both have to be individually active for H_2O_2 electrosynthesis. Indeed, alloying an active metal with another metal that is relatively inactive at the potentials applied can give discrete reactive sites surrounded by a relatively inert material.[172] For example, in PdAu alloys it is the Pd sites that perform initial $2e^-$ transfer to O_2; Au binds O_2 only weakly and cannot alone cleave the O–O bond, but gives too slow a reaction rate to be practically useful without the alloyed Pd.[173, 174] The reactivities of alloy catalysts are dependent on the spacing between the more active metal atoms, such that finely tuning the ratio of inactive to active metal affords a volcano-type relationship between H_2O_2 selectivity and composition (FIG. 4).

Aside from PdAu, computational studies have shown that Pt or Pd, when alloyed with a wide range of metals, afford catalysts that are very selective towards H_2O_2, with $PtSn_2$ approaching the peak of the theoretical activity volcano.[109] Unfortunately, the dissolution potential of many of these metals is more negative than the reduction potential for oxygen, and so operating conditions would lead to their dissolution out of the alloy, leaving behind a Pt or Pd shell. Taking stability into account leaves $PtHg_4$ as the optimal candidate. The same concept of active sites on a relatively inert substrate has been employed in the development of single atom catalysts,[175] which feature single atoms of an active metal such as Pt isolated on (or in) a

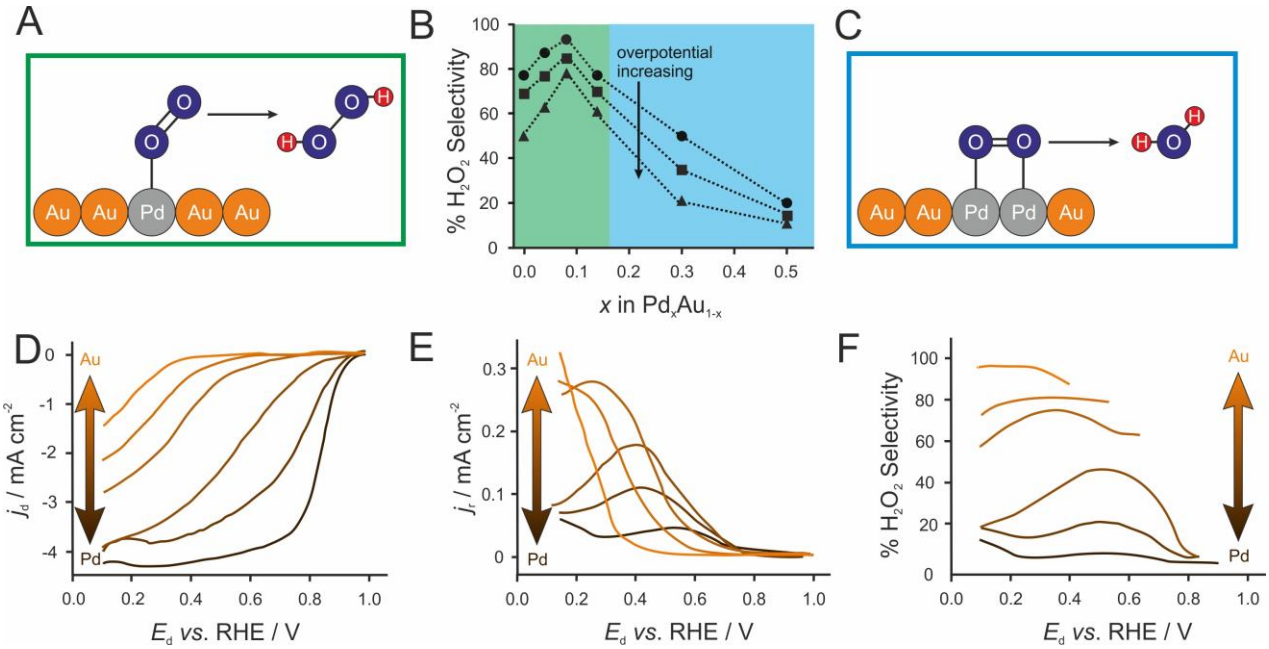

Figure 4 | **Selectivity in O_2 reduction to H_2O_2 as a function of Pd content in Pd_xAu_{1-x}. a** | The Pd(η^1-O_2) end-on binding mode is known as the Pauling model and is favoured when the Pd content is low. **b** | The selectivity towards H_2O_2 at 0 (circles), −0.1 (squares) and −0.2 V vs. saturated calomel electrode (triangles) depends on the alloy composition. The green region represents the low Pd region, in which H_2O_2 formation is favoured. The blue region represents the high Pd region, in which H_2O formation is favoured. **d–f** | Pd_xAu_{1-x} alloys can also be studied by immobilizing them on the disc electrode of a rotating ring–disc electrodes. **d** | The total current density at the electrode disc (j_d) for O_2 reduction as a function of disc potential E_d. **e** | The observed current density at the ring (j_r) corresponding to H_2O_2 detection. **f** | The corresponding selectivity for H_2O_2 for the given catalyst. In general, pure Pd exhibits the greatest current density but pure Au shows the best selectivity, highlighting how alloys give access to a compromise between the two. Part **b** was drawn from data in REF 142, parts **d–f** were drawn from data in REF 168.

relatively inactive support such as S-doped carbon[141] or TiN.[176] The Pt_1 active sites favour end-on O_2 binding over other binding modes, such that the selectivity for H_2O_2 generation can reach 95%.

One must never lose sight that optimizing selectivity typically has a detrimental effect on reaction rates. In the case of Pd_xAu_{1-x}, lower values of x will favour H_2O_2 selectivity but afford lower current densities. The ideal electrode material will represent a compromise — diluting the active material enhances selectivity but lowers the total rate of reaction. This present discussion of catalytic activity assumes that the system maintains its integrity under the operating conditions. Some materials are only kinetically stable, and PdAu nanoparticles, when subjected to oxidizing or reducing potentials, can undergo partial phase separation to afford a Au-rich or Pd-rich shell, respectively. These new materials have different selectivities towards H_2O_2,[177] highlighting the need to not only characterize activity but also the robustness of catalysts under operating conditions.

Carbon materials

Metal alloys have promising catalytic activities, but tend to include precious metals that are expensive and in limited availability. This has motivated the development of carbon materials as cheap and abundant electrocatalysts. The starting point for these materials can be one of a number of carbon allotropes, including graphite,[178-181] graphene,[182-184] C nanotubes,[135, 185, 186] as well as porous[137, 148, 187] and amorphous[188-190] C. Porous C materials can have high surface areas and enable efficient mass transport, but can also favour H_2O_2 by offering more defect sites than the uniform materials.[148] According to DFT calculations, certain defect configurations afford a material at pinnacle of the volcano plot for $2e^-$ O_2 reduction (FIG. 2), highlighting their role as active sites. In general, bulk coordinatively saturated C sites are less reactive than these defect sites. However, the optimum structure is not obvious because although a material with smaller pores has a higher density of defects, it also can lead to lower H_2O_2 yields because any H_2O_2 cannot easily diffuse from the electrode before undergoing further redox.[191]

In addition to modifying the structure of carbon electrode materials, one can also improve the performance of a H_2O_2 electrosynthesis catalyst by tuning the composition of the surface or bulk. For example, the current density of a H_2O_2-generating carbon material can be improved by oxidizing the surface anodically,[192, 193] or thermally[179] to provide a more active surface decorated with O and/or OH groups. In the case of carbon black, selectivity towards H_2O_2 formation can be substantially improved by annealing it to afford a more hydrophobic surface that favours the diffusion of O_2 to the electrode and helps to maintain the characteristic three-phase boundary that is responsible for fast reaction rates at gas diffusion electrodes.[194] As we noted, oxidized carbon materials bearing several $–CO_2H$ and –C–O–C– sites are predicted to have optimal activity for H_2O_2 formation.[108]

The activities of doped carbon materials are more dependent on the chemical effect of the dopant rather than the effects imparted on microstructure or defects.[184, 195] A wide range of dopants have been studied, including B,[131, 196] N,[197-199] P,[182, 184] S,[183, 200] F[201] and a number of transition metals.[202-206] Both mesoporous carbon and graphite, when doped with N atoms, can exhibit high selectivities towards H_2O_2.[207, 208] For example, a N-C framework containing triazine and viologen groups has many redox-active sites that can accept electrons and transfer them to O_2 to selectively give H_2O_2, even over an 8 h electrolysis.[198] An exception to this has been observed with carbon nanotubes, where N-doping causes the apparent number of transferred electrons to increase (from n = 1.8 to 3.9).[135]

Most transition metal dopants are not suitable for H_2O_2 electrosynthesis, and the selectivity of metal-doped carbon materials for H_2O_2 can decrease with increasing dopant concentration.[203, 205] Likewise, carbons with lower levels of N and Fe–N dopants have greater selectivities,[209] a result that is intuitive given that higher concentrations of active sites favour $4e^-$ ORR. One can obtain selective catalysts by immobilizing [M(porphyrinato)] or [M(phthalocyaninato)] complexes on a carbon support[139, 140, 210] but these materials undergo degradation in the presence of H_2O_2, making them unsuitable for long-term use.[205, 211]

Metal oxides

Metal oxides can produce H_2O_2 through either cathodic or anodic electrosynthesis (FIG. 5a,b). Ru and Ir oxides mediate the anodic reaction at the lowest reported overpotentials,[117, 212, 213] but are too expensive for large-scale applications[214] and tend to favour O_2 formation.[215-218] Most promising metal oxides include SnO_2,[62] MnO_x,[214, 219] WO_3-$BiVO_4$[220-222] and TiO_2.[223-227] Much of the literature dedicated to H_2O_2 synthesis from these materials is related to the overall photochemical reaction:[228]

$$O_2 + 2H_2O + h\nu \rightarrow 2H_2O_2 \quad (8)$$

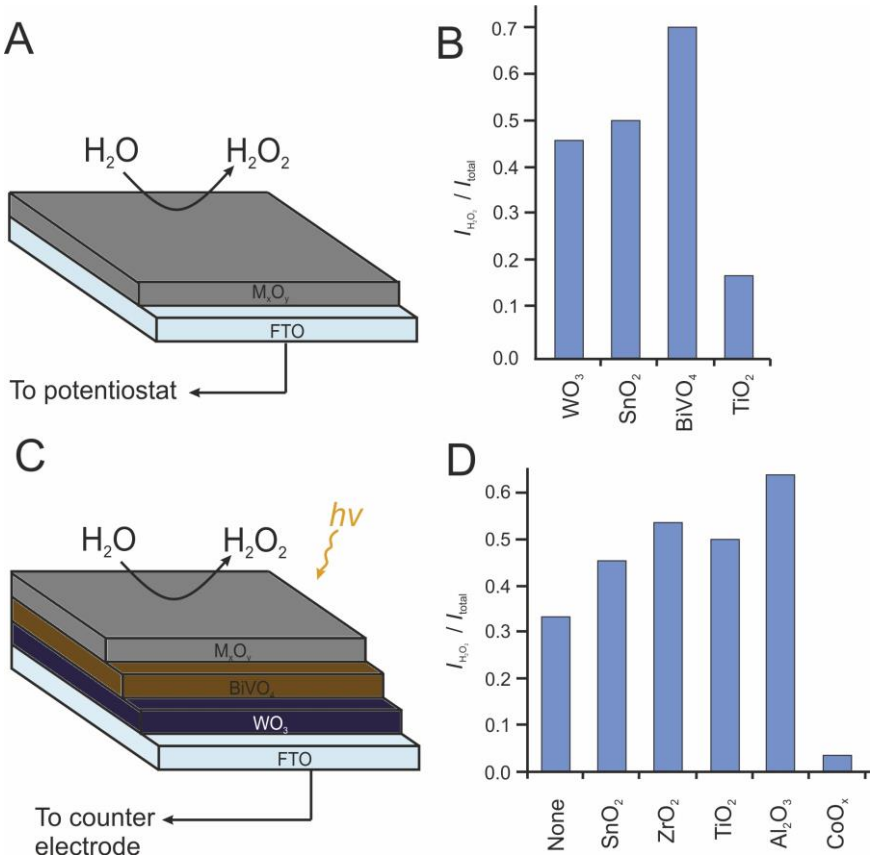

Figure 5. | **Metal-oxide-based electrodes and their performance in electrocatalytic and photoelectrocatalytic H_2O_2 production. a** | Schematic structure of a metal oxide electrode deposited on FTO glass and connected to a potentiostat. **b** | Each oxide has a different current efficiency, defined as the fraction of the total current density passed (j_{total}) used to oxidize H_2O to H_2O_2 ($j_{H_2O_2}$). Electrodes were used in the dark and biased at 2.3 V vs. RHE (WO_3), 3.1 V vs. RHE ($BiVO_4$ and SnO_2) and 3.3 V vs RHE (TiO_2). **c** | Schematic structure of WO_3-$BiVO_4$ deposited on FTO glass and coated with a metal oxide catalyst M_xO_y. The electrode is not potentially biased but is illuminated as part of a photovoltaic cell. **d** | The current efficiencies of illuminated photoelectrodes with different catalysts M_xO_y. Overall, high current efficiencies are observed for both electrochemically-driven and photochemically-driven reactions. Part **b** was drawn from data in REF [129]. Part **d** was drawn from data in REF 146. FTO, fluorine-doped tin oxide; RHE, reversible hydrogen electrode.

The process involves the initial absorption of a photon to trigger charge separation: a hole in the valence band (h_{vb}^+) and an electron in the conduction band (e_{cb}^-). These enable H_2O_2 generation both by H_2O oxidation and O_2 reduction.[225]

$$MO_x + h\nu \rightarrow h_{vb}^+ + e_{cb}^- \quad (9a)$$

$$2H_2O + 2h_{vb}^+ \rightarrow H_2O_2 + 2H^+ \quad (9b)$$

$$O_2 + 2e_{cb}^- + 2H^+ \rightarrow H_2O_2 \quad (9c)$$

Although the requirements for photocatalysts and electrochemical catalysts are expected to differ, exploiting both approaches simultaneously may afford a photoelectrode that forms H_2O_2 very efficiently.[129] Conflicting views exist regarding whether it is the reduction of O_2[229, 230] or the oxidation of H_2O[58] that is the predominant source of H_2O_2. Experiments in degassed solutions suggest that the former reaction is more prevalent [225, 231]

Present research into metal oxide catalysts for H_2O_2 electrosynthesis mostly focuses on refining the catalysts by changing their metal content. This can afford mixed-metal catalysts such as the ternary oxide $CaSnO_3$, which shows good selectivity for H_2O_2 and was stable over a 12 h electrolysis.[132]. Alternatively, catalysts can be tuned for H_2O_2 formation by stacking thin layers of different metal oxides. For example, modifying the surface of a WO_3-$BiVO_4$ electrode with other metal oxides increases selectivity towards H_2O_2 production,[228] with a combination of WO_3, $BiVO_4$ and Al_2O_3 being the optimal photoanode (FIG. 5c,d). This increase in selectivity during anodic H_2O_2 production is interesting given that previous works indicated that the purely photochemical reaction proceeds by a reduction step. Taken together, the mechanisms of the photocatalytic and electrocatalytic reactions are likely different.

Metal oxide electrodes are more commonly used for anodic H_2O_2 electrosynthesis than they are for

cathodic electrosynthesis, although a few suitable materials have been identified. These O_2 reduction catalysts typically take the form of metal oxide nanoparticles dispersed on C supports. A number of oxides have shown promise, including WO_3,[145] Co_xO_y,[232] CeO_2,[233-235] Ta_2O_5,[147, 236] Nb_2O_5[237] and V_xO_y.[238] The usefulness of these species for cathodic H_2O_2 electrosynthesis is limited because they are intrinsically efficient materials for the $4e^-$ ORR. Thus, their selectivity towards H_2O_2 can only come from physical engineering, such as loading a surface only sparsely with these oxides to lower the likelihood that H_2O_2 is reduced to O_2.[145, 235]

Although metal-oxide-based catalysts can have useful activities, their electrical conductivities are lower than metals. Indeed, many of the best performing metal oxide catalysts are semiconductors, and the potential drop across this layer will affect the potential at the electrode surface. Additionally, in the case of metal oxide nanoparticles on a support such as C, the conductivity of the metal oxide will affect the electrical contact between the particles and the support and electrode, which can introduce additional potential drops and detract from the performance of the electrode.

Electrolytes and additives

The number of electrons *n* accepted by each O_2 molecule decreases with increasing pH, to the point where basic solutions favour $n = 2$ and the formation of H_2O_2. Increasing $[OH^-]$ can poison an electrode surface, and the lower density of active sites favours end-on adsorption and precludes the deleterious reduction of H_2O_2.[239, 240] Unfortunately, OH^- can also catalyze the disproportionation of H_2O_2 (equation 4).[241, 242] Thus, one must make a compromise with pH — if it is too low then *n* increases towards 4, and if it is too high H_2O_2 undergoes decomposition.

With the above discussion in mind, it would make sense to deliberately partially poison an electrode surface with something other than OH^-. For example, Pt electrodes for O_2 reduction can be modified by exposing them to solutions containing Br^-,[243] I^-,[244] or Cl^-,[245] and even traces of these ligands can affect the surface.[245-247] Similarly, Pt can be poisoned by adding S or Se atoms.[248] Alternatively, Pt nanoparticles can be coated with a layer of porous amorphous carbon, which restricts substrate access and thereby favours end-on binding of O_2 and formation of H_2O_2 as the end product.[249] Partially poisoning an electrode will lower the current densities it can operate at because the electroactive area is lowered. This has motivated the development of alternative additives that do not detract from current density but can improve selectivity by affecting the kinetics at the electrode surface and slow down the reduction of H_2O_2. One option is to add halide salts of $N(alkyl)_4^+$, which not only affect the electrical double layer but also adsorb onto the electrode and raise the local pH, favouring localized H_2O_2 production.[250] The selectivity towards H_2O_2 was the same in $N(alkyl)_4Br$ and $N(alkyl)_4I$, so the cation effect was outweighing contributions from the halides. Only low concentrations of $N(alkyl)_4^+$ are needed, such that one can favour H_2O_2 without substantially increasing the bulk pH and catalyzing its decomposition.

H_2O_2 has a number of decomposition pathways, both through heterogeneous redox at an electrode (Equations 1 and 2) or through homogeneous reactions in bulk solution (Equations 4 and 7a). Heterogeneous decomposition can be slowed down by minimizing contact between H_2O_2 and the counter electrode by placing the latter in a separate cell compartment.[214, 251] Homogeneous decomposition is harder to prevent because the process can occur by homolysis or by reaction with radicals or OH^-. H_2O_2 decomposition can also be catalyzed by trace metal ions such as Fe^{2+}, which participates in the Fenton reaction (equation 10):[252-254]

$$Fe^{2+} + H_2O_2 \longrightarrow Fe^{3+} + HO^{\bullet} + OH^- \qquad (10)$$

One can avoid the Fenton reaction by trapping aqueous metal ions as catalytically inactive complexes, including those of chelating ligands such as 2-(*N*-anilino)ethanol or aminophosphonates.[254-257] The homolysis of H_2O_2 affords radicals that can proceed to react with H_2O_2:[258]

$$HO_2^{\bullet} + H_2O_2 \longrightarrow HO^{\bullet} + H_2O + O_2 \qquad (11a)$$

$$HO^{\bullet} + H_2O_2 \longrightarrow HO_2^{\bullet} + H_2O \qquad (11b)$$

It is possible to prevent these deleterious cascade reactions by trapping $HO^{\bullet}$ and $HO_2^{\bullet}$ with radical scavengers such as N-oxides or peracids.[259, 260] and to stop their formation in the first place by shielding the cell from the UV light that would otherwise facilitate H_2O_2 homolysis.[261] A distinct approach to avoiding H_2O_2 decomposition is to convert the product into a peroxosolvate salt, which can precipitate from solution and be stored as a stable solid and used as an on-demand oxidant or hydrolyzed back to H_2O_2.[262-264] As well as avoiding its decomposition, sequestering H_2O_2 shifts reaction equilibria towards H_2O_2 as the end

product. This requires separation of the peroxosolvate to isolate H_2O_2, although peroxosolvates have similar oxidizing properties to H_2O_2 and might be used directly in some applications.

Electrodes, reaction cells and their architecture

Complementary to research on developing catalyst materials with the ideal intrinsic properties is the equally important pursuit of engineering the catalyst and other cell components into an efficient device. The ideal electrode structure should have a sufficiently large number of adsorption sites, whilst also allowing H_2O_2 to rapidly desorb before it can undergo further reactions. The desorption of H_2O_2 is not only favoured when metal–H_2O_2 interactions are weak but also under conditions of fast mass transport. High surface areas and fast mass transport give rise to high current densities, which are particularly desirable when scaling up electrochemical cells from the laboratory scale to the industrial scale (FIG. 6).

A number of different electrode and cell designs tackle the same requirements in different ways. A popular choice for H_2O_2 electrosynthesis from O_2 is the gas diffusion electrode (GDE, FIG. 6a),[194, 265] which comprises a porous layer with a hydrophobic component, such as carbon paper impregnated with a hydrophobic polymer. The electrode acts as a membrane between the O_2-containing gas and the liquid electrolyte. The catalyst is deposited onto the GDE at the solid–liquid interface, so that when O_2 flows through the membrane it can be reduced as soon as it dissolves. Much of the research in this area has focused on the nature of the deposited catalyst, with metal nanoparticles being the most common choice. Care must be taken not to load the GDE with too much catalyst because this can physically hinder gas flow and lower the current density.[194] GDEs have a number of advantages over normal electrodes (those optimized for solutions) because mass transport in the gas phase is typically

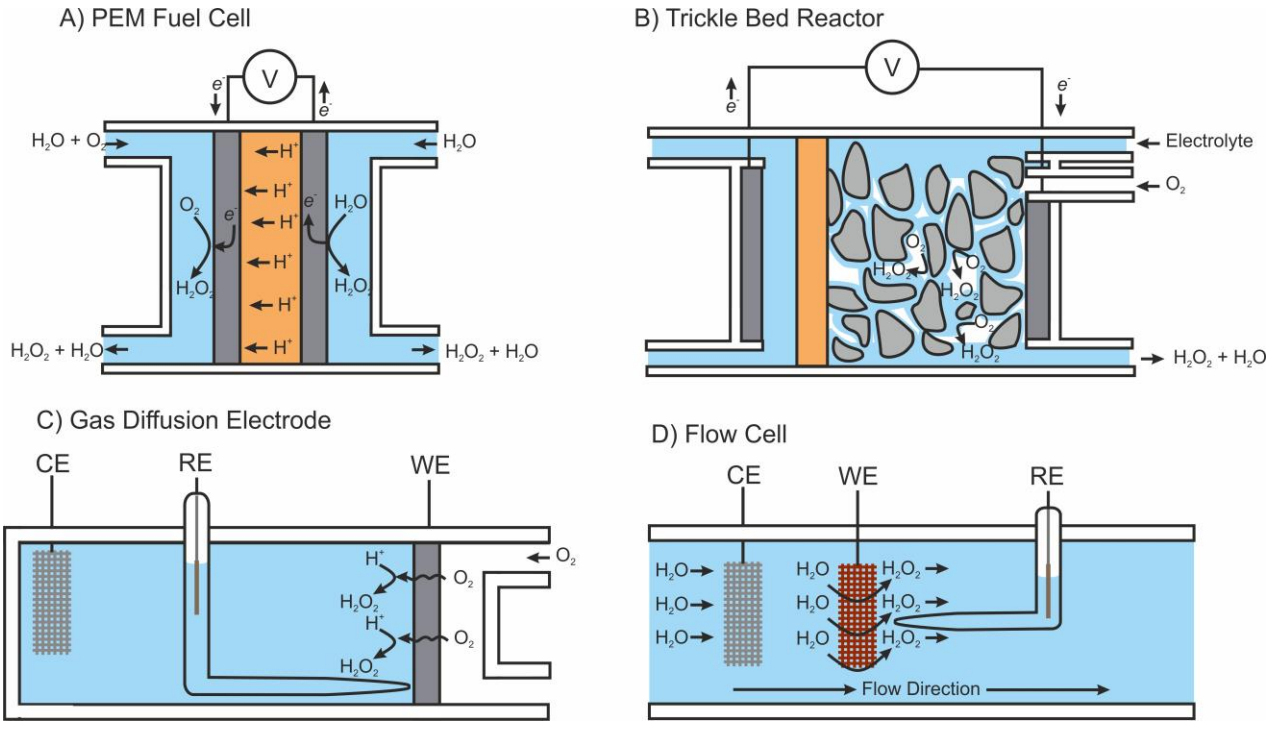

Figure 6. | **Possible cell configurations for the electrosynthesis of H_2O_2.** Blue regions denote liquid electrolyte, white regions denote gas flow, and orange regions represent conductive membranes. **a** | In a gas diffusion electrode, O_2 flows over the back of a porous hydrophobic electrode before being reduced at the solid–liquid interface. **b** | O_2 dissolved in an electrolyte can flow through or by a working electrode and be converted into H_2O_2. Electrodes such as foams or meshes have high surface areas and can give high current densities. Both the gas diffusion cell and flow cell can also be operated with a membrane dividing the solution into two compartments, with the CE in a separate compartment to the RE and WE. **c** | In a trickle bed reactor, the electrolyte and O_2 flow into the cathode chamber, which is packed with the catalyst. The electrolyte forms a thin film over the catalyst bed, so O_2 can dissolve and be rapidly reduced to H_2O_2. The H_2O_2 solution is then collected at the bottom of the reactor. The anodic chamber is often a flow chamber over a porous electrode to balance the charge. **d** | O_2 can be reduced at the cathode or H_2O oxidized at the anode to produce H_2O_2 in a PEM fuel cell. The two electrodes are separated by the PEM and flowing solution over the electrodes gives access to greater current densities. CE, counter electrode; RE, reference electrode; WE, working electrode; PEM, proton exchange membrane.

faster that it is in solution, and one does not need to consider the solubility limits of O_2 in the electrolyte.

We have described how a GDE can be suitable for the cathodic electrosynthesis of H_2O_2 because it can readily process the gaseous reactant O_2. When one instead considers anodic H_2O_2 electrosynthesis, it is still possible to have a similar effect by using a liquid flow cell (FIG. 6b). This can collect the product in a reservoir or circulate an intermediate to allow it to undergo further reactions within the same volume of solution to give a high concentration of the desired product. A number of distinct reaction environments are established when the solution flow is changed using arrangements like such as flow-by systems over parallel plate electrodes or flow-through systems using mesh or channel electrodes[266] These flow cells are particularly useful to assess a new material during its early development because they have well-defined mass transport regimes based on flow rate and geometry, such that setting up a reaction is relatively straightforward and is amenable to validation using finite element analysis.

Other reactor designs have been developed to increase overall currents by maximizing the active electrode area instead of mass transport. In the laboratory, this can be realized by using highly porous electrodes such as carbon felts or foams to offer large surface areas at which electrochemical reactions can occur.[4, 267] When scaled up, this concept takes the form of a trickle bed reactor, in which the electrode is a fixed bed of catalyst particles in a large chamber (FIG. 6c).[57, 268] The electrolyte is added into the top and then trickles down by gravity such that the effluent can be collected at the bottom. This combination of the large surface area and slow flow rate can afford concentrated solutions of H_2O_2[269-273]

Another reactor option is the proton exchange membrane (PEM, FIG. 6d) fuel cell.[60, 188, 210] In such a device, the anode and cathode are in two compartments separated by a H^+-conducting polymer membrane. These cells are effective for H_2O_2 electrosynthesis because the separation of the two electrodes means that H_2O_2 formed at the anode cannot be degraded at the cathode or vice versa. Electrochemical synthesis within a fuel cell presents the possibility of simultaneously harvesting electrical energy together with a useful product, which has clear energetic benefits, compared to standard synthesis that only consumes energy.[274]

If one separates the compartments in an electrochemical cell it is possible to simultaneously produce useful products at the anode and cathode and not have the products interact with each other. Perhaps the best known example of such a divergent paired electrochemical process is the chloralkali process, which generates Cl_2 and NaOH by oxidizing and reducing brine.[275] Many more examples of divergent processes exist, including the conversion of 4-(*t*-butyl)toluene to phthalide,[276] L-cystine to L-cysteine and L-cysteic acid,[277] dienes and CO_2 to diols and diacids[278] and O_2 and H_2O to H_2O_2 and oxidants such as O_3[279] or $HO^{\bullet}$.[280] An alternative approach is a convergent paired electrochemical process, in which the same product is generated in both compartments. This has been applied to the electrosynthesis of hydroquinone[281, 282] and glyoxylic acid.[283] Of course, concomitant cathodic and anodic H_2O_2 production from O_2 and H_2O is also possible, and encouragingly, a complete electrolysis cell operating at Faradaic efficiencies exceeding 90% has been patented.[284] This convergent paired process appears to be the most feasible approach for H_2O_2 electrosynthesis on an industrial scale.

Diverse reactor designs are used both in the academic literature and in industry. Numerous patents have been filed for reactor designs for H_2O_2 electrosynthesis. These are mostly based on the cathodic production of H_2O_2 from O_2 at a gas diffusion cathode in a PEM fuel cell, with the goal being to achieve give high mass transport rates and minimize the problems regarding the low solubility of O_2 in aqueous electrolytes.[285-287] By refining the design and orientation of the gas and liquid phase compartments, these have been incorporated into stackable, modular units, where the gas and liquid phases flow across multiple sequentially stacked gas diffusion electrodes, which greatly increases the overall output capacity.[288] Similar bipolar electrolyzers to those used in the chloralkali process have been used to generate useful products at both the cathode and anode, such as H_2O_2 and HOCl,[289] or H_2O_2 at both the anode and cathode.[290]

Future research needs

A key figure of merit that requires improvement continues to be the selectivity towards H_2O_2 over H_2O or O_2. The selectivity of catalysts is often reported at low overpotentials in the kinetically controlled regime, and these catalysts can give rise to low overall yields for high current density electrosynthesis. There is plenty of scope for the improvement of catalyst materials through changing substrate composition, architecture,

surface treatment or experimental design. A number of materials have come close to the theoretical maximum ($CaSnO_3$, WO_3 and $BiVO_4$ at the anode[129, 130, 132], PtHg and PdHg at the cathode[107, 109]), so these would be good candidates from which to further develop materials. The environmental concerns associated with Hg-based materials, and the costs and unsustainability related to using pure noble metals, mean that Pt or Au alloys[109, 142] or N-doped carbon materials[137, 197] are among the more practical candidates for cathode materials.

The redox activity of H_2O_2 makes 100% selectivity impossible. The presence of H_2O_2 adsorbed to electrode surfaces at large overpotentials means that some degree of further redox seems inevitable for both the anodic or cathodic mechanism. A more realistic aim would be to operate at a high selectivity (≈ 95% for example) while also stabilizing any H_2O_2 that forms and/or maximizing the current density. We reiterate that much of the available literature has described studies that focus on selectivity, with current density being relatively neglected in fundamental studies. A major challenge is to increase the current density of a H_2O_2 electrosynthesis cell without lowering selectivity, because, in general, a more active catalyst is also more likely to mediate the decomposition of H_2O_2 to O_2 and H_2O.

Once we can perform $2e^-$ redox to favour H_2O_2 in preference to the $4e^-$ ORR or OER, it will then be necessary to shift focus towards a desired working concentration of H_2O_2 within the experimental setup. This concentration will vary depending on application; solution phase alkene oxidation syntheses have been reported using between 1.5 and 4.5 equivalents of peroxide to alkene, where the exact ratio depends on the alkene and catalyst used.[291] This might be achieved by operating at high selectivity and low current density, or higher current density and lower selectivity. In this regard, the electrosynthesis of H_2O_2 has a substantial advantage over other synthesis methods because the side-products of the reaction are simply O_2 and H_2O. Thus, obtaining a high yield even at reduced selectivity is not a problem because it will not affect the purity of the resulting H_2O_2 solution.

Aside from catalytic activity, the practical value of any electrode material also depends on its long-term stability. One should repeatedly cycle the potential and also conduct controlled potential electrolysis over a long time. Following these, it is important to once again characterize the electrode morphology using microscopy techniques, and to look for any changes in the rate of H_2O_2 formation by complementary electrochemical or spectroscopic techniques. Repeated use of an electrode even at moderate overpotentials can cause the metal and metal oxide catalysts to degrade. Indeed, H_2O_2 itself can break down a number of potential catalyst materials. For example, although promising in terms of activity, metalloporphyrin-based species have revealed themselves to be insufficiently robust, even in relatively short-term experiments[139, 140] Other active materials may also prove unsuitable when subjected to more rigorous electrosynthesis trials conducted over hundreds of hours.

This Review has described different H_2O_2 electrosynthesis strategies from both cathodic and anodic directions. On the face of it, there appears to be no clear preference between these options, except perhaps that because the anodic route uses H_2O as the starting material it is easier to realize practically because it does not require the same level of solution aeration as the cathodic route. The distinction between the two directions is more about what happens at the counter electrode, something that is often not considered during electrochemistry, so long as a sufficient current can be passed and no disruptive side-products are generated. However, a growing number of researchers are now designing paired electrochemical processes for the production of useful materials at both the anode and the cathode.[281, 292] Thus, the choice of anodic or cathodic H_2O_2 electrosynthesis is dependent on the additional product that is desired; anodic H_2O_2 electrosynthesis also provides H_2,[220, 222] whereas cathodic H_2O_2 electrosynthesis can generate O_2 or O_3.[279] Likewise, the oxidation of $2H_2O$ or H_2O_2 can be coupled to reduction of CO_2 to HCO_2H or C_2H_4. Organic products might later be combined with H_2O_2 to give other useful products.[293, 294] As mentioned in the preceding section, one can also design a cell purely for electrochemical synthesis of H_2O_2, which forms simultaneously at the anode and the cathode.[228, 290]

The emphasis of H_2O_2 electrosynthesis research should be guided by the application for which the H_2O_2 product is intended. The various applications of aqueous H_2O_2 will each require a certain H_2O_2 concentration and may only tolerate a certain pH range. If we consider a plausible end goal of online H_2O_2 electrosynthesis, in which electrosynthesized H_2O_2 is immediately consumed en route to a value-added product, it is important that H_2O_2 can be synthesized at a comparable rate and at a concentration in a solvent/solute mixture appropriate for its final use. For example, if the

second reaction is alkane oxidation, a big challenge is to produce H_2O_2 in sufficiently high concentrations to drive the effect the oxidation. Thus, instead of using a separate reactor for the second step it may be advantageous to conduct a one-pot synthesis, in which H_2O_2 is formed in the presence of the organic to be oxidized. This would favour alkane oxidation because H_2O_2 would be abundant at the electrode surface (it would be more difficult to achieve the necessary concentrations in a bulk phase to be delivered to a second reactor). H_2O_2 can also be used for H_2O treatment because its catalytic decomposition by Fe cations effects the oxidation of organic impurities to less harmful products. This process is best performed at low pH in order to favour radical reactions and prevent precipitation of the catalytic Fe cations as hydroxides.[295, 296] If H_2O_2 is to be used in situ for the Fenton reaction, the candidate catalysts are limited to the small fraction of catalysts that are known to be efficient in acidic media. Otherwise, a workup strategy must be found, involving an acidification step while the solution is moved from the first reactor to the second.

Long-term goals for H_2O_2 electrosynthesis are likely to focus on scalability — moving from benchtop experiments to syntheses on industrially relevant scales. Many of the necessary reaction cells and architectures already exist for other reactions and could be easily adapted to H_2O_2 electrosynthesis. Up-scaling would most likely require increased stability of catalyst materials in concentrated H_2O_2. Alternatively, modifications could be made to the industrial rig, such as incorporating a flow system to remove H_2O_2 from the electrode to give added protection. Of course, the efficiency with which electrochemistry can afford useful dilute solutions of H_2O_2 means that we do not necessarily have the same high yield requirements as present industrial methods.

When considering the advancement of H_2O_2 electrosynthesis in the industry, it is unfortunate that an electrochemical engineering approach has not been described in most studies published. These studies neglect to target a certain reaction environment, as can be done by considering fluid flow, mass transport and current distribution. Only in this way can scale-up and industrial integration of electrochemical systems be possible. Advances in the achievable H_2O_2 production rates are coming through the use of porous 3D electrodes decorated with catalysts such as coated metal or carbon mesh, felt, foam or fibres.[297-299] Optimizing the channel depth, width and orientation within specifically designed flow fields can maximize the exposure of electrodes to the reactant — either H_2O through liquid flow over the anode or O_2 by gas flow over the cathode. Fundamental research into new catalyst materials for H_2O_2 electrosynthesis will find more relevance if it includes expanded analysis in which the entire reaction environment is considered in order to make materials ready for wide applications.

Conclusions

A diverse range of electrode materials is available for the electrochemical synthesis of H_2O_2. For cathodic electrosynthesis, carbon-based electrodes perform well because of their poor efficiency for the $4e^-$ ORR. The efficiency with which these catalysts produce H_2O_2 can be further improved by adding dopants or metal nanoparticles. For the anodic route, metal oxides such as $CaSnO_3$, $BiVO_4$ and WO_3 perform well. Many of these materials were originally developed as photocatalysts but can still give impressive yields without illumination. Accordingly, there is much scope for further improvement of these materials to enhance the H_2O_2 yield by focusing on selectivity and/or current density. The choice of cathodic or anodic synthesis becomes more important when considering the reaction occurring at the counter electrode. Thus, H_2O_2 and another product can be formed in paired electrochemical processes or H_2O_2 can form at both the anode and cathode as part of dual electrosynthesis. The majority of papers published describe only short-term studies on model electrodes in laboratory electrolytes, so it is important to establish whether electrodes can exhibit long-term performance. Thus, one must consider their volumetric area, activity, resistance to degradation and their suitability to practical scale-up and industrial processing.

References

1. Hage, R. and Lienke, A., Applications of Transition-Metal Catalysts to Textile and Wood-Pulp Bleaching *Angew. Chem. Int. Ed.*, **45**, 206-222 (2006).
2. Raj, C. B. C. and Li Quen, H., Advanced Oxidation Processes for Wastewater Treatment: Optimization of UV/H_2O_2 Process through a Statistical Technique *Chem. Eng. Sci.*, **60**, 5305-5311 (2005).
3. Kosaka, K., *et al.*, Evaluation of the Treatment Performance of a Multistage Ozone/Hydrogen Peroxide Process by Decomposition by-Products *Water Res.*, **35**, 3587-3594 (2001).
4. Alvarez-Gallegos, A. and Pletcher, D., The Removal of Low Level Organics Via Hydrogen Peroxide Formed in a Reticulated Vitreous Carbon Cathode Cell, Part 1. The Electrosynthesis of Hydrogen Peroxide in

Aqueous Acidic Solutions *Electrochim. Acta*, **44**, 853-861 (1998).
5. Ponce de León, C. and Pletcher, D., Removal of Formaldehyde from Aqueous Solutions Via Oxygen Reduction Using a Reticulated Vitreous Carbon Cathode Cell *J. Appl. Electrochem.*, **25**, 307-314 (1995).
6. Tanev, P. T., Chibwe, M. and Pinnavaia, T. J., Titanium-Containing Mesoporous Molecular Sieves for Catalytic Oxidation of Aromatic Compounds *Nature*, **368**, 321 (1994).
7. Clerici, M. G. and Ingallina, P., Epoxidation of Lower Olefins with Hydrogen Peroxide and Titanium Silicalite *J. Catal.*, **140**, 71-83 (1993).
8. Noyori, R., Aoki, M. and Sato, K., Green Oxidation with Aqueous Hydrogen Peroxide *Chem. Commun.*, **0**, 1977-1986 (2003).
9. Lane, B. S. and Burgess, K., Metal-Catalyzed Epoxidations of Alkenes with Hydrogen Peroxide *Chem. Rev.*, **103**, 2457-2474 (2003).
10. Chua, S.-C., Xu, X. and Guo, Z., Emerging Sustainable Technology for Epoxidation Directed toward Plant Oil-Based Plasticizers *Process Biochem.*, **47**, 1439-1451 (2012).
11. Ma, J., Choudhury, N. A. and Sahai, Y., A Comprehensive Review of Direct Borohydride Fuel Cells *Renew. Sust. Energ. Rev.*, **14**, 183-199 (2010).
12. Ponce de León, C., Walsh, F. C., Pletcher, D., Browning, D. J. and Lakeman, J. B., Direct Borohydride Fuel Cells *J. Power Sources*, **155**, 172-181 (2006).
13. Campos-Martin, J. M., Blanco-Brieva, G. and Fierro, J. L. G., Hydrogen Peroxide Synthesis: An Outlook Beyond the Anthraquinone Process *Angew. Chem. Int. Ed.*, **45**, 6962-6984 (2006).
14. Santacesaria, E., Di Serio, M., Velotti, R. and Leone, U., Kinetics, Mass Transfer, and Palladium Catalyst Deactivation in the Hydrogenation Step of the Hydrogen Peroxide Synthesis Via Anthraquinone *Ind. Eng. Chem. Res.*, **33**, 277-284 (1994).
15. Cheng, Y., Wang, L., Lü, S., Wang, Y. and Mi, Z., Gas−Liquid−Liquid Three-Phase Reactive Extraction for the Hydrogen Peroxide Preparation by Anthraquinone Process *Ind. Eng. Chem. Res.*, **47**, 7414-7418 (2008).
16. Edwards, J. K. and Hutchings, G. J., Palladium and Gold–Palladium Catalysts for the Direct Synthesis of Hydrogen Peroxide *Angew. Chem. Int. Ed.*, **47**, 9192-9198 (2008).
17. Palmer, M. J., Musker, A. J., Roberts, G. T. and Ponce de León, C., A Method of Ranking Candidate Catalyst for the Decomposition of Hydrogen Peroxide, in *Space Propulsion 2010*, San Sebastian (2010).
18. Kosydar, R., Drelinkiewicz, A. and Ganhy, J. P., Degradation Reactions in Anthraquinone Process of Hydrogen Peroxide Synthesis *Catal. Lett.*, **139**, 105-113 (2010).
19. Sandelin, F., Oinas, P., Salmi, T., Paloniemi, J. and Haario, H., Kinetics of the Recovery of Active Anthraquinones *Ind. Eng. Chem. Res.*, **45**, 986-992 (2006).
20. Edwards, J. K., *et al.*, Switching Off Hydrogen Peroxide Hydrogenation in the Direct Synthesis Process *Science*, **323**, 1037-1041 (2009).
21. Edwards, J. K., Freakley, S. J., Lewis, R. J., Pritchard, J. C. and Hutchings, G. J., Advances in the Direct Synthesis of Hydrogen Peroxide from Hydrogen and Oxygen *Catal. Today*, **248**, 3-9 (2015).
22. Samanta, C., Direct Synthesis of Hydrogen Peroxide from Hydrogen and Oxygen: An Overview of Recent Developments in the Process *Appl. Catal., A*, **350**, 133-149 (2008).
23. Dittmeyer, R., Grunwaldt, J. D. and Pashkova, A., A Review of Catalyst Performance and Novel Reaction Engineering Concepts in Direct Synthesis of Hydrogen Peroxide *Catal. Today*, **248**, 149-159 (2015).
24. Adányi, N., Barna, T., Emri, T., Miskei, M. and Pócsi, I.,Hydrogen Peroxide Producing and Decomposing Enzymes: Their Use in Biosensors and Other Applications in *Industrial Enzymes: Structure, Function and Applications*, Polaina, J. and MacCabe, A. P. Editors, p. 441-459, Springer Netherlands, Dordrecht (2007).
25. Fantinato, S., Pollegioni, L. and Pilone, M. S., Engineering, Expression and Purification of a His-Tagged Chimeric D-Amino Acid Oxidase from Rhodotorula Gracilis *Enzyme Microb. Technol.*, **29**, 407-412 (2001).
26. Smart, E. J. and Anderson, R. G. W.,Alterations in Membrane Cholesterol That Affect Structure and Function of Caveolae in *Methods Enzymol.*, Sen, C. K. and Packer, L. Editors, p. 131-139, Academic Press, London (2002).
27. Perry, S. C., Gateman, S. M., Sifakis, J., Pollegioni, L. and Mauzeroll, J., Enhancement of the Enzymatic Biosensor Response through Targeted Electrode Surface Roughness *J. Electrochem. Soc.*, **165**, G3074-G3079 (2018).
28. Polcari, D., Perry, S. C., Pollegioni, L., Geissler, M. and Mauzeroll, J., Localized Detection of D-Serine by Using an Enzymatic Amperometric Biosensor and Scanning Electrochemical Microscopy *ChemElectroChem*, **4**, 920-926 (2017).
29. Massa, S., *et al.*, Growth Inhibition by Glucose Oxidase System of Enterotoxic Escherichia Coli and Salmonella Derby: In Vitro Studies *World J. Microbiol. Biotechnol.*, **17**, 287-291 (2001).
30. Traube, M., About the Electrolytic Formation of Hydrogen Peroxide at the Cathode *Ber. Kgl. Akad. Wiss. Berlin*, **2**, 1041-1050 (1887).

31. Manchot, W. and Herzog, J., Die Autoxydation Des Hydrazobenzols *Justus Liebigs Ann. Chem.*, **316**, 331-332 (1901).
32. Walton, J. H. and Filson, G. W., The Direct Preparation of Hydrogen Peroxide in a High Concentration *J. Am. Chem. Soc.*, **54**, 3228-3229 (1932).
33. Jones, C. W., *Applications of Hydrogen Peroxide and Derivatives*, Royal Society of Chemistry, Cambridge (1999).
34. Yi, Y., Wang, L., Li, G. and Guo, H., A Review on Research Progress in the Direct Synthesis of Hydrogen Peroxide from Hydrogen and Oxygen: Noble-Metal Catalytic Method, Fuel-Cell Method and Plasma Method *Catal. Sci. Technol.*, **6**, 1593-1610 (2016).
35. Berl, E., A New Cathodic Process for the Production of H_2O_2 *Trans. Electrochem. Soc.*, **76**, 359-369 (1939).
36. de Beco, P., Sur Les Réactions d'Oxydation au Pôle Positif dans l'Électrolyse par Éntincelle *C. R. Acad. Sci. (Paris)*, **207**, 623-625 (1938).
37. de Beco, P., l'Éctrolyse par Éntincelle II, Reactions au Pôle Positif *Bull. Soc. Chim. Fr.*, **12**, 789-792 (1945).
38. Davies, R. A. and Hickling, A., Glow-Discharge Electrolysis. Part I. The Anodic Formation of Hydrogen Peroxide in Inert Electrolytes *J. Chem. Soc. (London)*, 3595-3602 (1952).
39. Berl, W. G., A Reversible Oxygen Electrode *Trans. Electrochem. Soc.*, **83**, 253-270 (1943).
40. Patrick, W. A. and Wagner, H. B., Mechanism of Oxygen Reduction at an Iron Cathode *Corrosion*, **6**, 34-38 (1950).
41. Weisz, R. S. and Jaffe, S. S., The Mechanism of the Reduction of Oxygen at the Air Electrode *J. Electrochem. Soc.*, **93**, 128-141 (1948).
42. Mizuno, S., The Electrolytic Synthesis of Hydrogen Peroxide. II. On the Electrolysis Conditions *Denki Kagaku*, **17**, 288 (1949).
43. Mizuno, S., Studies on the Electrolytic Synthesis. I. Electrolytic Synthesis of Hydrogen Peroxide *Denki Kagaku*, **17**, 17 (1949).
44. Thénard, L. J., Observations sur des Nouvelles Combinaisons Entre l'Oxigène et Divers Acides *Ann. Chim. Phys.*, **8**, 306-312 (1818).
45. Bredig, G. and von Berneck, R. M., Über Anorganische Fermente. I. Über Platinkatalyse und die Chemische Dynamik des Wasserstoffsuperoxyds *Z. Phys. Chem.*, **31**, 258 (1899).
46. Schönbein, C. F., Die Zersetzungsverhältnisse des Ersten Salpetersäurehydrats, Verglichen mit Denen des Wasserstoffsuperoxyds und des Ozons *J. Prakt. Chem.*, **37**, 129-143 (1846).
47. Schönbein, C. F., Ueber die Chemische Polarisation des Sauerstoffs *J. Prakt. Chem.*, **78**, 63-93 (1859).
48. Schönbein, C. F., Chemische Mittheilungen *J. Prakt. Chem.*, **86**, 65-99 (1862).
49. Schönbein, C. F., Weitere Beiträge zur Nähern Kenntniss des Sauerstoffs *J. Prakt. Chem.*, **93**, 24-60 (1864).
50. Traube, M., Ueber Aktivirung des Sauerstoffs *Ber. Dtsch. Chem. Ges.*, **15**, 659-675 (1882).
51. Traube, M., Ueber die Aktivirung des Sauerstoffs *Ber. Dtsch. Chem. Ges.*, **15**, 2434-2443 (1882).
52. Comyns, A. E., *Encyclopedic Dictionary of Named Processes in Chemical Technology*, CRC Press (2014).
53. Henkel, H. and Weber, W. Manufacture of Hydrogen Peroxide. US Patent 1,108,752 (1914)
54. Henkel, H. Cathodic Production of Hydrogen Peroxide. German Patent 266,516 (1913)
55. Oloman, C. and Watkinson, A. P., The Electroreduction of Oxygen to Hydrogen Peroxide on Fluidized Cathodes *Can. J. Chem. Eng.*, **53**, 268-273 (1975).
56. Balej, J., Balogh, K. and Špalek, O., Possibility of Producing Hydrogen Peroxide by Cathodic Reduction of Oxygen *Chem. Pap. - Chem. Zvesti*, **30**, 384-392 (1976).
57. Oloman, C., Trickle Bed Electrochemical Reactors *J. Electrochem. Soc.*, **126**, 1885-1892 (1979).
58. Rao, M. V., Rajeshwar, K., Verneker, V. R. P. and DuBow, J., Photosynthetic Production of Hydrogen and Hydrogen Peroxide on Semiconducting Oxide Grains in Aqueous Solutions *J. Phys. Chem.*, **84**, 1987-1991 (1980).
59. McIntyre, J. A. and Phillips, R. F. Method for Electrolytic Production of Alkaline Peroxide Solutions. US Patent US4431494 (1984)
60. Otsuka, K. and Yamanaka, I., One Step Synthesis of Hydrogen Peroxide through Fuel Cell Reaction *Electrochim. Acta*, **35**, 319-322 (1990).
61. Viswanathan, V., Hansen, H. A., Rossmeisl, J. and Nørskov, J. K., Unifying the $2e^-$ and $4e^-$ Reduction of Oxygen on Metal Surfaces *J. Phys. Chem. Lett.*, **3**, 2948-2951 (2012).
62. Viswanathan, V., Hansen, H. A. and Nørskov, J. K., Selective Electrochemical Generation of Hydrogen Peroxide from Water Oxidation *J. Phys. Chem. Lett.*, **6**, 4224-4228 (2015).
63. Giomo, M., *et al.*, A Small-Scale Pilot Plant Using an Oxygen-Reducing Gas-Diffusion Electrode for Hydrogen Peroxide Electrosynthesis *Electrochim. Acta*, **54**, 808-815 (2008).
64. Kolyagin, G. A. and Kornienko, V. L., Pilot Laboratory Electrolyzer for Electrosynthesis of Hydrogen Peroxide in Acid and Alkaline Solutions *Russ. J. Appl. Chem.*, **84**, 68-71 (2011).
65. Kolyagin, G. A., Kornienko, V. L., Kudenko, Y. A., Tikhomirov, A. A. and Trifonov, S. V.,

Electrosynthesis of Hydrogen Peroxide from Oxygen in a Gas-Diffusion Electrode in Solutions of Mineralized Exometabolites *Russ. J. Electrochem.*, **49**, 1004-1007 (2013).
66. Tang, M. C.-Y., Wong, K.-Y. and Chan, T. H., Electrosynthesis of Hydrogen Peroxide in Room Temperature Ionic Liquids and in Situ Epoxidation of Alkenes *Chem. Commun.*, 1345-1347 (2005).
67. Li, W., Tian, M., Du, H. and Liang, Z., A New Approach for Epoxidation of Fatty Acids by a Paired Electrosynthesis *Electrochem. Commun.*, **54**, 46-50 (2015).
68. Chaenko, N. V., Kornienko, G. V. and Kornienko, V. L., Indirect Electrosynthesis of Peracetic Acid Using Hydrogen Peroxide Generated in Situ in a Gas Diffusion Electrode *Russ. J. Electrochem.*, **47**, 230-233 (2011).
69. González-García, J., Drouin, L., Banks, C. E., Šljukić, B. and Compton, R. G., At Point of Use Sono-Electrochemical Generation of Hydrogen Peroxide for Chemical Synthesis: The Green Oxidation of Benzonitrile to Benzamide *Ultrason. Sonochem.*, **14**, 113-116 (2007).
70. Song, C. and Zhang, J.,Electrocatalytic Oxygen Reduction Reaction in *PEM Fuel Cell Electrocatalysts and Catalyst Layers: Fundamentals and Applications*, Zhang, J. Editor, p. 89-134, Springer, London (2008).
71. Wroblowa, H. S., Yen Chi, P. and Razumney, G., Electroreduction of Oxygen: A New Mechanistic Criterion *J. Electroanal. Chem.*, **69**, 195-201 (1976).
72. Noël, J.-M., Latus, A., Lagrost, C., Volanschi, E. and Hapiot, P., Evidence for OH Radical Production During Electrocatalysis of Oxygen Reduction on Pt Surfaces: Consequences and Application *J. Am. Chem. Soc.*, **134**, 2835-2841 (2012).
73. Shao, M.-h., Liu, P. and Adžić, R. R., Superoxide Anion Is the Intermediate in the Oxygen Reduction Reaction on Platinum Electrodes *J. Am. Chem. Soc.*, **128**, 7408-7409 (2006).
74. Bard, A. J., Parsons, R. and Jordan, J., *Standard Potentials in Aqueous Solution*, M. Dekker, New York, NY (1985).
75. Li, Y., *et al.*, Superoxide Decay Pathways in Oxygen Reduction Reaction on Carbon-Based Catalysts Evidenced by Theoretical Calculations *ChemSusChem*, **12**, 1133-1138 (2019).
76. Gara, M., *et al.*, Oxygen Reduction at Sparse Arrays of Platinum Nanoparticles in Aqueous Acid: Hydrogen Peroxide as a Liberated Two Electron Intermediate *Phys. Chem. Chem. Phys.*, **15**, 19487-19495 (2013).
77. Dong, J.-C., *et al.*, In Situ Raman Spectroscopic Evidence for Oxygen Reduction Reaction Intermediates at Platinum Single-Crystal Surfaces *Nat. Energy*, **4**, 60-67 (2019).
78. Grgur, B. N., Marković, N. M. and Ross, P. N., Temperature-Dependent Oxygen Electrochemistry on Platinum Low-Index Single Crystal Surfaces in Acid Solutions *Can. J. Chem.*, **75**, 1465-1471 (1997).
79. Keith, J. A. and Jacob, T., Theoretical Studies of Potential-Dependent and Competing Mechanisms of the Electrocatalytic Oxygen Reduction Reaction on Pt(111) *Angew. Chem. Int. Ed.*, **49**, 9521-9525 (2010).
80. Sidik, R. A. and Anderson, A. B., Density Functional Theory Study of O_2 Electroreduction when Bonded to a Pt Dual Site *J. Electroanal. Chem.*, **528**, 69-76 (2002).
81. Tripkovic, V. and Vegge, T., Potential- and Rate-Determining Step for Oxygen Reduction on Pt(111) *J. Phys. Chem. C*, **121**, 26785-26793 (2017).
82. Jinnouchi, R., Kodama, K., Hatanaka, T. and Morimoto, Y., First Principles Based Mean Field Model for Oxygen Reduction Reaction *Phys. Chem. Chem. Phys.*, **13**, 21070-21083 (2011).
83. Viswanathan, V., Hansen, H. A., Rossmeisl, J. and Nørskov, J. K., Universality in Oxygen Reduction Electrocatalysis on Metal Surfaces *ACS Catal.*, **2**, 1654-1660 (2012).
84. Gómez-Marín, A. M., Rizo, R. and Feliu, J. M., Oxygen Reduction Reaction at Pt Single Crystals: A Critical Overview *Catal. Sci. Technol.*, **4**, 1685-1698 (2014).
85. Ignaczak, A., Santos, E. and Schmickler, W., Oxygen Reduction Reaction on Gold in Alkaline Solutions – the Inner or Outer Sphere Mechanisms in the Light of Recent Achievements *Current Opinion in Electrochemistry* (2018).
86. Griffith, J. S., On the Magnetic Properties of Some Haemoglobin Complexes *Proc. R. Soc. London, Ser. A*, **235**, 23 (1956).
87. Adžić, R. R.,Recent Advances in the Kinetics of Oxygen Reduction in *Electrocatalysis*, Lipkowski, J. and Ross, P. N. Editors, p. 197-242, John Wiley & Sons, Ltd, New York, NY (1998).
88. Yeager, E., Razaq, M., Gervasio, D., Razaq, A. and Tryk, D.,The Electrolyte Factor in O_2 Reduction Electrocatalysis in *Proceedings of the Workshop on Structural Effects in Electrocatalysis and Oxygen Electrochemistry*, Scherson, D., Tryk, D., Daroux, M. and Xing, X. Editors, p. 440-474, Electrochemical Society, Pennington, NJ (1992).
89. Gattrell, M. and MacDougall, B.,Reaction Mechanisms of the O_2 Reduction/Evolution Reaction in *Handbook of Fuel Cells*, Vielstich, W., Lamm, A., Gasteiger, H. A. and Yokokawa, H. Editors, p. 443-464, John Wiley & Sons, Ltd, New York, NY (2010).
90. Nørskov, J. K., *et al.*, Origin of the Overpotential for Oxygen Reduction at a Fuel-

Cell Cathode *J. Phys. Chem. B*, **108**, 17886-17892 (2004).
91. Perry, S. C. and Denuault, G., Transient Study of the Oxygen Reduction Reaction on Reduced Pt and Pt Alloys Microelectrodes: Evidence for the Reduction of Pre-Adsorbed Oxygen Species Linked to Dissolved Oxygen *Phys. Chem. Chem. Phys.*, **17**, 30005-30012 (2015).
92. Perry, S. C. and Denuault, G., The Oxygen Reduction Reaction (ORR) on Reduced Metals: Evidence for a Unique Relationship between the Coverage of Adsorbed Oxygen Species and Adsorption Energy *Phys. Chem. Chem. Phys.*, **18**, 10218-10223 (2016).
93. Greeley, J., *et al.*, Alloys of Platinum and Early Transition Metals as Oxygen Reduction Electrocatalysts *Nat. Chem.*, **1**, 552 (2009).
94. Hammer, B., Special Sites at Noble and Late Transition Metal Catalysts *Top. Catal.*, **37**, 3-16 (2006).
95. Kitchin, J. R., Nørskov, J. K., Barteau, M. A. and Chen, J. G., Modification of the Surface Electronic and Chemical Properties of Pt(111) by Subsurface 3d Transition Metals *J. Chem. Phys.*, **120**, 10240-10246 (2004).
96. Stamenković, V., Schmidt, T. J., Ross, P. N. and Marković, N. M., Surface Composition Effects in Electrocatalysis: Kinetics of Oxygen Reduction on Well-Defined Pt_3Ni and Pt_3Co Alloy Surfaces *J. Phys. Chem. B*, **106**, 11970-11979 (2002).
97. Mukerjee, S., Srinivasan, S., Soriaga, M. P. and McBreen, J., Role of Structural and Electronic Properties of Pt and Pt Alloys on Electrocatalysis of Oxygen Reduction: An in Situ Xanes and Exafs Investigation *J. Electrochem. Soc.*, **142**, 1409-1422 (1995).
98. Spanos, I., Dideriksen, K., Kirkensgaard, J. J. K., Jelavic, S. and Arenz, M., Structural Disordering of De-Alloyed Pt Bimetallic Nanocatalysts: The Effect on Oxygen Reduction Reaction Activity and Stability *Phys. Chem. Chem. Phys.*, **17**, 28044-28053 (2015).
99. Jalan, V. and Taylor, E. J., Importance of Interatomic Spacing in Catalytic Reduction of Oxygen in Phosphoric Acid *J. Electrochem. Soc.*, **130**, 2299-2302 (1983).
100. Stamenković, V. R., *et al.*, Trends in Electrocatalysis on Extended and Nanoscale Pt-Bimetallic Alloy Surfaces *Nat. Mater.*, **6**, 241 (2007).
101. Lee, K. R., Jung, Y. and Woo, S. I., Combinatorial Screening of Highly Active Pd Binary Catalysts for Electrochemical Oxygen Reduction *ACS Comb. Sci.*, **14**, 10-16 (2012).
102. Gentil, R. and Villullas, H. M., Oxygen Reduction Activity and Methanol Tolerance of Carbon-Supported PtV Nanoparticles and the Effects of Heat Treatment at Low Temperatures *J. Solid State Electrochem.*, **20**, 1119-1129 (2016).
103. Xin, H., Holewinski, A. and Linic, S., Predictive Structure–Reactivity Models for Rapid Screening of Pt-Based Multimetallic Electrocatalysts for the Oxygen Reduction Reaction *ACS Catal.*, **2**, 12-16 (2012).
104. Stamenković, V. R., *et al.*, Improved Oxygen Reduction Activity on $Pt_3Ni(111)$ via Increased Surface Site Availability *Science*, **315**, 493-497 (2007).
105. Suntivich, J., May, K. J., Gasteiger, H. A., Goodenough, J. B. and Shao-Horn, Y., A Perovskite Oxide Optimized for Oxygen Evolution Catalysis from Molecular Orbital Principles *Science*, **334**, 1383-1385 (2011).
106. Vojvodic, A. and Nørskov, J. K., Optimizing Perovskites for the Water-Splitting Reaction *Science*, **334**, 1355-1356 (2011).
107. Verdaguer-Casadevall, A., *et al.*, Trends in the Electrochemical Synthesis of H_2O_2: Enhancing Activity and Selectivity by Electrocatalytic Site Engineering *Nano Lett.*, **14**, 1603-1608 (2014).
108. Lu, Z., *et al.*, High-Efficiency Oxygen Reduction to Hydrogen Peroxide Catalysed by Oxidized Carbon Materials *Nat. Catal.*, **1**, 156-162 (2018).
109. Siahrostami, S., *et al.*, Enabling Direct H_2O_2 Production through Rational Electrocatalyst Design *Nat. Mater.*, **12**, 1137 (2013).
110. Hansen, H. A., Viswanathan, V. and Nørskov, J. K., Unifying Kinetic and Thermodynamic Analysis of 2 e^- and 4 e^- Reduction of Oxygen on Metal Surfaces *J. Phys. Chem. C*, **118**, 6706-6718 (2014).
111. Seh, Z. W., *et al.*, Combining Theory and Experiment in Electrocatalysis: Insights into Materials Design *Science*, **355** (2017).
112. Khorshidi, A., Violet, J., Hashemi, J. and Peterson, A. A., How Strain Can Break the Scaling Relations of Catalysis *Nat. Catal.*, **1**, 263-268 (2018).
113. Montemore, M. M. and Medlin, J. W., Scaling Relations between Adsorption Energies for Computational Screening and Design of Catalysts *Catal. Sci. Technol.*, **4**, 3748-3761 (2014).
114. Calle-Vallejo, F., Krabbe, A. and García-Lastra, J. M., How Covalence Breaks Adsorption-Energy Scaling Relations and Solvation Restores Them *Chem. Sci.*, **8**, 124-130 (2017).
115. Siahrostami, S., Björketun, M. E., Strasser, P., Greeley, J. and Rossmeisl, J., Tandem Cathode for Proton Exchange Membrane Fuel Cells *Phys. Chem. Chem. Phys.*, **15**, 9326-9334 (2013).
116. Singh, A. and Spiccia, L., Water Oxidation Catalysts Based on Abundant 1st Row Transition Metals *Coord. Chem. Rev.*, **257**, 2607-2622 (2013).
117. Walter, M. G., *et al.*, Solar Water Splitting Cells *Chem. Rev.*, **110**, 6446-6473 (2010).

118. Burke, M. S., Enman, L. J., Batchellor, A. S., Zou, S. and Boettcher, S. W., Oxygen Evolution Reaction Electrocatalysis on Transition Metal Oxides and (Oxy)Hydroxides: Activity Trends and Design Principles *Chem. Mater.*, **27**, 7549-7558 (2015).
119. Reier, T., Oezaslan, M. and Strasser, P., Electrocatalytic Oxygen Evolution Reaction (OER) on Ru, Ir, and Pt Catalysts: A Comparative Study of Nanoparticles and Bulk Materials *ACS Catal.*, **2**, 1765-1772 (2012).
120. Cheng, Y. and Jiang, S. P., Advances in Electrocatalysts for Oxygen Evolution Reaction of Water Electrolysis-from Metal Oxides to Carbon Nanotubes *Prog. Nat. Sci. Mater.*, **25**, 545-553 (2015).
121. Busch, M., *et al.*, Beyond the Top of the Volcano? – A Unified Approach to Electrocatalytic Oxygen Reduction and Oxygen Evolution *Nano Energy*, **29**, 126-135 (2016).
122. Su, H.-Y., *et al.*, Identifying Active Surface Phases for Metal Oxide Electrocatalysts: A Study of Manganese Oxide Bi-Functional Catalysts for Oxygen Reduction and Water Oxidation Catalysis *Phys. Chem. Chem. Phys.*, **14**, 14010-14022 (2012).
123. Blakemore, J. D., Gray, H. B., Winkler, J. R. and Müller, A. M., Co_3O_4 Nanoparticle Water-Oxidation Catalysts Made by Pulsed-Laser Ablation in Liquids *ACS Catal.*, **3**, 2497-2500 (2013).
124. Maitra, U., Naidu, B. S., Govindaraj, A. and Rao, C. N. R., Importance of Trivalency and the e_g^1 Configuration in the Photocatalytic Oxidation of Water by Mn and Co Oxides *Proc. Natl. Acad. Sci. U.S.A.*, **110**, 11704-11707 (2013).
125. Mattioli, G., Giannozzi, P., Amore Bonapasta, A. and Guidoni, L., Reaction Pathways for Oxygen Evolution Promoted by Cobalt Catalyst *J. Am. Chem. Soc.*, **135**, 15353-15363 (2013).
126. Smith, R. D. L., Prévot, M. S., Fagan, R. D., Trudel, S. and Berlinguette, C. P., Water Oxidation Catalysis: Electrocatalytic Response to Metal Stoichiometry in Amorphous Metal Oxide Films Containing Iron, Cobalt, and Nickel *J. Am. Chem. Soc.*, **135**, 11580-11586 (2013).
127. Busch, M., Ahlberg, E. and Panas, I., Validation of Binuclear Descriptor for Mixed Transition Metal Oxide Supported Electrocatalytic Water Oxidation *Catal. Today*, **202**, 114-119 (2013).
128. Lee, Y., Suntivich, J., May, K. J., Perry, E. E. and Shao-Horn, Y., Synthesis and Activities of Rutile IrO_2 and RuO_2 Nanoparticles for Oxygen Evolution in Acid and Alkaline Solutions *J. Phys. Chem. Lett.*, **3**, 399-404 (2012).
129. Shi, X., *et al.*, Understanding Activity Trends in Electrochemical Water Oxidation to Form Hydrogen Peroxide *Nat. Commun.*, **8**, 701 (2017).
130. Siahrostami, S., Li, G.-L., Viswanathan, V. and Nørskov, J. K., One- or Two-Electron Water Oxidation, Hydroxyl Radical, or H_2O_2 Evolution *J. Phys. Chem. Lett.*, **8**, 1157-1160 (2017).
131. Chen, S., *et al.*, Designing Boron Nitride Islands in Carbon Materials for Efficient Electrochemical Synthesis of Hydrogen Peroxide *J. Am. Chem. Soc.*, **140**, 7851-7859 (2018).
132. Park, S. Y., *et al.*, $CaSnO_3$: An Electrocatalyst for Two-Electron Water Oxidation Reaction to Form H_2O_2 *ACS Energy Lett.*, **4**, 352-357 (2019).
133. Mizuno, S., Activated Carbon Electrodes for the Electrolytic Synthesis of Hydrogen Peroxide. I. Conditions Necessary for the Electrode Production. *Bull. Tokyo Inst. Technol.*, **13**, 102 (1948).
134. Ignatenko, E. and Barmashenko, I., Cathode Preparation of Hydrogen Peroxide *Zh. Prikl. Khim.*, **37**, 2415 (1964).
135. Gong, K., Du, F., Xia, Z., Durstock, M. and Dai, L., Nitrogen-Doped Carbon Nanotube Arrays with High Electrocatalytic Activity for Oxygen Reduction *Science*, **323**, 760-764 (2009).
136. Kornienko, V. L., Kolyagin, G. A., Kornienko, G. V., Parfenov, V. A. and Ponomarenko, I. V., Electrosynthesis of H_2O_2 from O_2 in a Gas-Diffusion Electrode Based on Mesostructured Carbon Cmk-3 *Russ. J. Electrochem.*, **54**, 258-264 (2018).
137. Sun, Y., *et al.*, Efficient Electrochemical Hydrogen Peroxide Production from Molecular Oxygen on Nitrogen-Doped Mesoporous Carbon Catalysts *ACS Catal.*, **8**, 2844-2856 (2018).
138. Thostenson, J. O., *et al.*, Enhanced H_2O_2 Production at Reductive Potentials from Oxidized Boron-Doped Ultrananocrystalline Diamond Electrodes *ACS Appl. Mater. Interfaces*, **9**, 16610-16619 (2017).
139. Barros, W. R. P., Reis, R. M., Rocha, R. S. and Lanza, M. R. V., Electrogeneration of Hydrogen Peroxide in Acidic Medium Using Gas Diffusion Electrodes Modified with Cobalt (II) Phthalocyanine *Electrochim. Acta*, **104**, 12-18 (2013).
140. Silva, F. L., Reis, R. M., Barros, W. R. P., Rocha, R. S. and Lanza, M. R. V., Electrogeneration of Hydrogen Peroxide in Gas Diffusion Electrodes: Application of Iron (II) Phthalocyanine as a Modifier of Carbon Black *J. Electroanal. Chem.*, **722-723**, 32-37 (2014).
141. Choi, C. H., *et al.*, Tuning Selectivity of Electrochemical Reactions by Atomically

Dispersed Platinum Catalyst *Nat. Commun.*, **7**, 10922 (2016).
142. Jirkovský, J. S., *et al.*, Single Atom Hot-Spots at Au–Pd Nanoalloys for Electrocatalytic H_2O_2 Production *J. Am. Chem. Soc.*, **133**, 19432-19441 (2011).
143. Antonin, V. S., *et al.*, Synthesis and Characterization of Nanostructured Electrocatalysts Based on Nickel and Tin for Hydrogen Peroxide Electrogeneration *Electrochim. Acta*, **109**, 245-251 (2013).
144. Pinheiro, V. S., *et al.*, Ceria High Aspect Ratio Nanostructures Supported on Carbon for Hydrogen Peroxide Electrogeneration *Electrochim. Acta*, **259**, 865-872 (2018).
145. Assumpção, M. H. M. T., *et al.*, Low Tungsten Content of Nanostructured Material Supported on Carbon for the Degradation of Phenol *Appl. Catal., B*, **142-143**, 479-486 (2013).
146. Fuku, K., Miyase, Y., Miseki, Y., Gunji, T. and Sayama, K., WO_3/$BiVO_4$ Photoanode Coated with Mesoporous Al_2O_3 Layer for Oxidative Production of Hydrogen Peroxide from Water with High Selectivity *RSC Adv.*, **7**, 47619-47623 (2017).
147. Xu, A., *et al.*, Electrogeneration of Hydrogen Peroxide Using Ti/IrO_2–Ta_2O_5 Anode in Dual Tubular Membranes Electro-Fenton Reactor for the Degradation of Tricyclazole without Aeration *Chem. Eng. J.*, **295**, 152-159 (2016).
148. Chen, S., *et al.*, Defective Carbon-Based Materials for the Electrochemical Synthesis of Hydrogen Peroxide *ACS Sustain. Chem. Eng.*, **6**, 311-317 (2018).
149. Rouhet, M., Bozdech, S., Bonnefont, A. and Savinova, E. R., Influence of the Proton Transport on the Orr Kinetics and on the H_2O_2 Escape in Three-Dimensionally Ordered Electrodes *Electrochem. Commun.*, **33**, 111-114 (2013).
150. Maruyama, J., Inaba, M. and Ogumi, Z., Rotating Ring-Disk Electrode Study on the Cathodic Oxygen Reduction at Nafion®-Coated Gold Electrodes *J. Electroanal. Chem.*, **458**, 175-182 (1998).
151. Marković, N. M., Gasteiger, H. A. and Ross, P. N., Oxygen Reduction on Platinum Low-Index Single-Crystal Surfaces in Sulfuric Acid Solution: Rotating Ring-Pt(hkl) Disk Studies *J. Phys. Chem.*, **99**, 3411-3415 (1995).
152. Zečević, S., Dražić, D. M. and Gojković, S., Oxygen Reduction on Iron: Part III. An Analysis of the Rotating Disk-Ring Electrode Measurements in near Neutral Solutions *J. Electroanal. Chem.*, **265**, 179-193 (1989).
153. Shih, Y.-H., Sagar, G. V. and Lin, S. D., Effect of Electrode Pt Loading on the Oxygen Reduction Reaction Evaluated by Rotating Disk Electrode and Its Implication on the Reaction Kinetics *J. Phys. Chem. C*, **112**, 123-130 (2008).
154. Sánchez-Sánchez, C. M. and Bard, A. J., Hydrogen Peroxide Production in the Oxygen Reduction Reaction at Different Electrocatalysts as Quantified by Scanning Electrochemical Microscopy *Anal. Chem.*, **81**, 8094-8100 (2009).
155. Sánchez-Sánchez, C. M., Rodríguez-López, J. and Bard, A. J., Scanning Electrochemical Microscopy. 60. Quantitative Calibration of the Secm Substrate Generation/Tip Collection Mode and Its Use for the Study of the Oxygen Reduction Mechanism *Anal. Chem.*, **80**, 3254-3260 (2008).
156. Shen, Y., Träuble, M. and Wittstock, G., Detection of Hydrogen Peroxide Produced During Electrochemical Oxygen Reduction Using Scanning Electrochemical Microscopy *Anal. Chem.*, **80**, 750-759 (2008).
157. Dobrzeniecka, A., *et al.*, Application of Secm in Tracing of Hydrogen Peroxide at Multicomponent Non-Noble Electrocatalyst Films for the Oxygen Reduction Reaction *Catal. Today*, **202**, 55-62 (2013).
158. Johnson, L. and Walsh, D. A., Tip Generation–Substrate Collection–Tip Collection Mode Scanning Electrochemical Microscopy of Oxygen Reduction Electrocatalysts *J. Electroanal. Chem.*, **682**, 45-52 (2012).
159. Pletcher, D. and Sotiropoulos, S., A Study of Cathodic Oxygen Reduction at Platinum Using Microelectrodes *J. Electroanal. Chem.*, **356**, 109-119 (1993).
160. Birkin, P. R., Elliott, J. M. and Watson, Y. E., Electrochemical Reduction of Oxygen on Mesoporous Platinum Microelectrodes *Chemical Communications*, 1693-1694 (2000).
161. Sheng, H., Ji, H., Ma, W., Chen, C. and Zhao, J., Direct Four-Electron Reduction of O_2 to H_2O on TiO_2 Surfaces by Pendant Proton Relay *Angew. Chem. Int. Ed.*, **52**, 9686-9690 (2013).
162. Liu, C. L., Hu, C.-C., Wu, S.-H. and Wu, T.-H., Electron Transfer Number Control of the Oxygen Reduction Reaction on Nitrogen-Doped Reduced-Graphene Oxides Using Experimental Design Strategies *J. Electrochem. Soc.*, **160**, H547-H552 (2013).
163. Zhou, R., Zheng, Y., Jaroniec, M. and Qiao, S.-Z., Determination of the Electron Transfer Number for the Oxygen Reduction Reaction: From Theory to Experiment *ACS Catal.*, **6**, 4720-4728 (2016).
164. Chen, S. and Kucernak, A., Electrocatalysis under Conditions of High Mass Transport Rate: Oxygen Reduction on Single Submicrometer-Sized Pt Particles Supported on Carbon *J. Phys. Chem. B*, **108**, 3262-3276 (2004).
165. Taylor, S., Fabbri, E., Levecque, P., Schmidt, T. J. and Conrad, O., The Effect of Platinum Loading and Surface Morphology on Oxygen Reduction Activity *Electrocatalysis*, **7**, 287-296 (2016).

166. Ilea, P., Dorneanu, S. and Popescu, I. C., Electrosynthesis of Hydrogen Peroxide by Partial Reduction of Oxygen in Alkaline Media. Part II: Wall-Jet Ring Disc Electrode for Electroreduction of Dissolved Oxygen on Graphite and Glassy Carbon *J. Appl. Electrochem.*, **30**, 187-192 (2000).
167. von Weber, A., Baxter, E. T., White, H. S. and Anderson, S. L., Cluster Size Controls Branching between Water and Hydrogen Peroxide Production in Electrochemical Oxygen Reduction at Pt_n/ITO *J. Phys. Chem. C*, **119**, 11160-11170 (2015).
168. Pizzutilo, E., *et al.*, Electrocatalytic Synthesis of Hydrogen Peroxide on Au-Pd Nanoparticles: From Fundamentals to Continuous Production *Chem. Phys. Lett.*, **683**, 436-442 (2017).
169. Félix-Navarro, R. M., *et al.*, Pt–Pd Bimetallic Nanoparticles on Mwcnts: Catalyst for Hydrogen Peroxide Electrosynthesis *J. Nanopart. Res.*, **15**, 1802 (2013).
170. Antonin, V. S., *et al.*, W@Au Nanostructures Modifying Carbon as Materials for Hydrogen Peroxide Electrogeneration *Electrochim. Acta*, **231**, 713-720 (2017).
171. Erikson, H., *et al.*, Oxygen Electroreduction on Electrodeposited PdAu Nanoalloys *Electrocatalysis*, **6**, 77-85 (2015).
172. Shao, M., Palladium-Based Electrocatalysts for Hydrogen Oxidation and Oxygen Reduction Reactions *J. Power Sources*, **196**, 2433-2444 (2011).
173. Rodriguez, P. and Koper, M. T. M., Electrocatalysis on Gold *Phys. Chem. Chem. Phys.*, **16**, 13583-13594 (2014).
174. Marković, N. M., Adić, R. R. and Vešović, V. B., Structural Effects in Electrocatalysis: Oxygen Reduction on the Gold Single Crystal Electrodes with (110) and (111) Orientations *J. Electroanal. Chem.*, **165**, 121-133 (1984).
175. Liu, J., Bunes, B. R., Zang, L. and Wang, C., Supported Single-Atom Catalysts: Synthesis, Characterization, Properties, and Applications *Environmental Chemistry Letters*, **16**, 477-505 (2018).
176. Yang, S., Kim, J., Tak, Y. J., Soon, A. and Lee, H., Single-Atom Catalyst of Platinum Supported on Titanium Nitride for Selective Electrochemical Reactions *Angew. Chem. Int. Ed.*, **55**, 2058-2062 (2016).
177. Jirkovský, J. S., Panas, I., Romani, S., Ahlberg, E. and Schiffrin, D. J., Potential-Dependent Structural Memory Effects in Au–Pd Nanoalloys *J. Phys. Chem. Lett.*, **3**, 315-321 (2012).
178. Miao, J., Zhu, H., Tang, Y., Chen, Y. and Wan, P., Graphite Felt Electrochemically Modified in H_2SO_4 Solution Used as a Cathode to Produce H_2O_2 for Pre-Oxidation of Drinking Water *Chem. Eng. J.*, **250**, 312-318 (2014).
179. Wang, Y., *et al.*, Preparation and Characterization of a Novel KOH Activated Graphite Felt Cathode for the Electro-Fenton Process *Appl. Catal., B*, **165**, 360-368 (2015).
180. Yu, F., Zhou, M. and Yu, X., Cost-Effective Electro-Fenton Using Modified Graphite Felt That Dramatically Enhanced on H_2O_2 Electro-Generation without External Aeration *Electrochim. Acta*, **163**, 182-189 (2015).
181. Zhou, L., *et al.*, Electrogeneration of Hydrogen Peroxide for Electro-Fenton System by Oxygen Reduction Using Chemically Modified Graphite Felt Cathode *Sep. Purif. Technol.*, **111**, 131-136 (2013).
182. Zhao, Z., Li, M., Zhang, L., Dai, L. and Xia, Z., Design Principles for Heteroatom-Doped Carbon Nanomaterials as Highly Efficient Catalysts for Fuel Cells and Metal–Air Batteries *Adv. Mater.*, **27**, 6834-6840 (2015).
183. Zhao, Z. and Xia, Z., Design Principles for Dual-Element-Doped Carbon Nanomaterials as Efficient Bifunctional Catalysts for Oxygen Reduction and Evolution Reactions *ACS Catal.*, **6**, 1553-1558 (2016).
184. Zhao, Z., Zhang, L. and Xia, Z., Electron Transfer and Catalytic Mechanism of Organic Molecule-Adsorbed Graphene Nanoribbons as Efficient Catalysts for Oxygen Reduction and Evolution Reactions *J. Phys. Chem. C*, **120**, 2166-2175 (2016).
185. Zhang, X., Fu, J., Zhang, Y. and Lei, L., A Nitrogen Functionalized Carbon Nanotube Cathode for Highly Efficient Electrocatalytic Generation of H_2O_2 in Electro-Fenton System *Sep. Purif. Technol.*, **64**, 116-123 (2008).
186. Kozlova, L. S., Novikov, V. T., Garaeva, G. R., Gol'din, M. M. and Kolesnikov, V. A., Electrodes Modified with Carbon Materials in Electrosynthesis of the Dissolved Hydrogen Peroxide Solutions and Their Medical Properties *Prot. Met. Phys. Chem. Surf.*, **51**, 985-989 (2015).
187. Valim, R. B., *et al.*, Electrogeneration of Hydrogen Peroxide in Gas Diffusion Electrodes Modified with Tert-Butyl-Anthraquinone on Carbon Black Support *Carbon*, **61**, 236-244 (2013).
188. Lobyntseva, E., Kallio, T., Alexeyeva, N., Tammeveski, K. and Kontturi, K., Electrochemical Synthesis of Hydrogen Peroxide: Rotating Disk Electrode and Fuel Cell Studies *Electrochim. Acta*, **52**, 7262-7269 (2007).
189. Pérez, J. F., *et al.*, Electrochemical Jet-Cell for the in-Situ Generation of Hydrogen Peroxide *Electrochem. Commun.*, **71**, 65-68 (2016).
190. Ilea, P., Dorneanu, S. and Nicoară, A., Hydrogen Peroxide Electrosynthesis by Partial Oxygen Reduction in Alkaline Media. I: Voltammetric Study on Unmodified Carbonaceous Materials *Rev. Roum. Chim.*, **44**, 555-561 (1999).

191. Park, J., Nabae, Y., Hayakawa, T. and Kakimoto, M.-a., Highly Selective Two-Electron Oxygen Reduction Catalyzed by Mesoporous Nitrogen-Doped Carbon *ACS Catal.*, **4**, 3749-3754 (2014).
192. Potapova, G. F., Kasatkin, E. V., Panesh, A. M., Lozovskii, A. D. and Kozlova, N. V., Hydrogen Peroxide Electrosynthesis on Nonplatinum Materials *Russ. J. Electrochem.*, **40**, 1193-1197 (2004).
193. Vlaic, C. and Dorneanu, S., Galvanostatic Graphite Electroactivation for Hydrogen Peroxide Electrosynthesis by Multi-Sequence and Auto-Adaptive Techniques *Studia UBB Chemia*, **60**, 141-150 (2015).
194. Pérez, J. F., *et al.*, Improving the Efficiency of Carbon Cloth for the Electrogeneration of H_2O_2: Role of Polytetrafluoroethylene and Carbon Black Loading *Ind. Eng. Chem. Res.*, **56**, 12588-12595 (2017).
195. Chai, G.-L., Hou, Z., Ikeda, T. and Terakura, K., Two-Electron Oxygen Reduction on Carbon Materials Catalysts: Mechanisms and Active Sites *J. Phys. Chem. C*, **121**, 14524-14533 (2017).
196. Coria, G., Pérez, T., Sirés, I. and Nava, J. L., Mass Transport Studies During Dissolved Oxygen Reduction to Hydrogen Peroxide in a Filter-Press Electrolyzer Using Graphite Felt, Reticulated Vitreous Carbon and Boron-Doped Diamond as Cathodes *J. Electroanal. Chem.*, **757**, 225-229 (2015).
197. Xia, G., Lu, Y. and Xu, H., Electrogeneration of Hydrogen Peroxide for Electro-Fenton Via Oxygen Reduction Using Polyacrylonitrile-Based Carbon Fiber Brush Cathode *Electrochim. Acta*, **158**, 390-396 (2015).
198. Peng, L.-Z., *et al.*, Highly Effective Electrosynthesis of Hydrogen Peroxide from Oxygen on a Redox-Active Cationic Covalent Triazine Network *Chem. Commun.*, **54**, 4433-4436 (2018).
199. Iglesias, D., *et al.*, N-Doped Graphitized Carbon Nanohorns as a Forefront Electrocatalyst in Highly Selective O_2 Reduction to H_2O_2 *Chem*, **4**, 106-123 (2018).
200. Perazzolo, V., *et al.*, Nitrogen and Sulfur Doped Mesoporous Carbon as Metal-Free Electrocatalysts for the in Situ Production of Hydrogen Peroxide *Carbon*, **95**, 949-963 (2015).
201. Zhao, K., *et al.*, Enhanced H_2O_2 Production by Selective Electrochemical Reduction of O_2 on Fluorine-Doped Hierarchically Porous Carbon *J. Catal.*, **357**, 118-126 (2018).
202. Nabae, Y., *et al.*, The Role of Fe in the Preparation of Carbon Alloy Cathode Catalysts *ECS Trans.*, **25**, 463-467 (2009).
203. Lefèvre, M. and Dodelet, J.-P., Fe-Based Catalysts for the Reduction of Oxygen in Polymer Electrolyte Membrane Fuel Cell Conditions: Determination of the Amount of Peroxide Released During Electroreduction and Its Influence on the Stability of the Catalysts *Electrochim. Acta*, **48**, 2749-2760 (2003).
204. Nallathambi, V., Lee, J.-W., Kumaraguru, S. P., Wu, G. and Popov, B. N., Development of High Performance Carbon Composite Catalyst for Oxygen Reduction Reaction in PEM Proton Exchange Membrane Fuel Cells *J. Power Sources*, **183**, 34-42 (2008).
205. Bezerra, C. W. B., *et al.*, A Review of Fe–N/C and Co–N/C Catalysts for the Oxygen Reduction Reaction *Electrochim. Acta*, **53**, 4937-4951 (2008).
206. Kusoru, T., Nakamatsu, S., Nishiki, Y., Tanaka, M. and Wakita, S. Process for Producing Acidic Water Containing Dissolved Hydrogen Peroxide and Electrolytic Cell Therefor. Europe Patent EP 0 949 205 A1 (1999)
207. Fellinger, T.-P., Hasché, F., Strasser, P. and Antonietti, M., Mesoporous Nitrogen-Doped Carbon for the Electrocatalytic Synthesis of Hydrogen Peroxide *J. Am. Chem. Soc.*, **134**, 4072-4075 (2012).
208. Sidik, R. A., Anderson, A. B., Subramanian, N. P., Kumaraguru, S. P. and Popov, B. N., O_2 Reduction on Graphite and Nitrogen-Doped Graphite: Experiment and Theory *J. Phys. Chem. B*, **110**, 1787-1793 (2006).
209. Muthukrishnan, A., Nabae, Y., Okajima, T. and Ohsaka, T., Kinetic Approach to Investigate the Mechanistic Pathways of Oxygen Reduction Reaction on Fe-Containing N-Doped Carbon Catalysts *ACS Catal.*, **5**, 5194-5202 (2015).
210. Yamanaka, I., *et al.*, Electrocatalysis of Heat-Treated Cobalt-Porphyrin/Carbon for Hydrogen Peroxide Formation *Electrochim. Acta*, **108**, 321-329 (2013).
211. Schulenburg, H., *et al.*, Catalysts for the Oxygen Reduction from Heat-Treated Iron(III) Tetramethoxyphenylporphyrin Chloride: Structure and Stability of Active Sites *J. Phys. Chem. B*, **107**, 9034-9041 (2003).
212. Wang, L., Duan, L., Tong, L. and Sun, L., Visible Light-Driven Water Oxidation Catalyzed by Mononuclear Ruthenium Complexes *J. Catal.*, **306**, 129-132 (2013).
213. Badiei, Y. M., *et al.*, Water Oxidation with Mononuclear Ruthenium(II) Polypyridine Complexes Involving a Direct Ru^{IV}=O Pathway in Neutral and Alkaline Media *Inorg. Chem.*, **52**, 8845-8850 (2013).
214. McDonnell-Worth, C. and MacFarlane, D. R., Ion Effects in Water Oxidation to Hydrogen Peroxide *RSC Adv.*, **4**, 30551-30557 (2014).
215. Guan, J., *et al.*, Synthesis and Demonstration of Subnanometric Iridium Oxide as Highly Efficient and Robust Water Oxidation Catalyst *ACS Catal.*, **7**, 5983-5986 (2017).

216. Kim, S., Cho, M. and Lee, Y., Iridium Oxide Dendrite as a Highly Efficient Dual Electro-Catalyst for Water Splitting and Sensing of H_2O_2 *J. Electrochem. Soc.*, **164**, B3029-B3035 (2017).
217. Iqbal, M. N., *et al.*, Mesoporous Ruthenium Oxide: A Heterogeneous Catalyst for Water Oxidation *ACS Sustain. Chem. Eng.*, **5**, 9651-9656 (2017).
218. Gustafson, K. P. J., *et al.*, Water Oxidation Mediated by Ruthenium Oxide Nanoparticles Supported on Siliceous Mesocellular Foam *Catal. Sci. Technol.*, **7**, 293-299 (2017).
219. Izgorodin, A., Izgorodina, E. and MacFarlane, D. R., Low Overpotential Water Oxidation to Hydrogen Peroxide on a MnO_x Catalyst *Energy Environ. Sci.*, **5**, 9496-9501 (2012).
220. Fuku, K., *et al.*, Photoelectrochemical Hydrogen Peroxide Production from Water on a $WO_3/BiVO_4$ Photoanode and from O_2 on an Au Cathode without External Bias *Chem. Asian J.*, **12**, 1111-1119 (2017).
221. Fuku, K., Miyase, Y., Miseki, Y., Gunji, T. and Sayama, K., Enhanced Oxidative Hydrogen Peroxide Production on Conducting Glass Anodes Modified with Metal Oxides *ChemistrySelect*, **1**, 5721-5726 (2016).
222. Fuku, K. and Sayama, K., Efficient Oxidative Hydrogen Peroxide Production and Accumulation in Photoelectrochemical Water Splitting Using a Tungsten Trioxide/Bismuth Vanadate Photoanode *Chem. Commun.*, **52**, 5406-5409 (2016).
223. Goto, H., Hanada, Y., Ohno, T. and Matsumura, M., Quantitative Analysis of Superoxide Ion and Hydrogen Peroxide Produced from Molecular Oxygen on Photoirradiated TiO_2 Particles *J. Catal.*, **225**, 223-229 (2004).
224. Hirakawa, T., Yawata, K. and Nosaka, Y., Photocatalytic Reactivity for O_2^- and OH Radical Formation in Anatase and Rutile TiO_2 Suspension as the Effect of H_2o_2 Addition *Appl. Catal., A*, **325**, 105-111 (2007).
225. Cai, R., Kubota, Y. and Fujishima, A., Effect of Copper Ions on the Formation of Hydrogen Peroxide from Photocatalytic Titanium Dioxide Particles *J. Catal.*, **219**, 214-218 (2003).
226. Zhang, J. and Nosaka, Y., Quantitative Detection of OH Radicals for Investigating the Reaction Mechanism of Various Visible-Light TiO_2 Photocatalysts in Aqueous Suspension *J. Phys. Chem. C*, **117**, 1383-1391 (2013).
227. Sánchez-Quiles, D. and Tovar-Sánchez, A., Sunscreens as a Source of Hydrogen Peroxide Production in Coastal Waters *Environ. Sci. Technol.*, **48**, 9037-9042 (2014).
228. Mase, K., Yoneda, M., Yamada, Y. and Fukuzumi, S., Efficient Photocatalytic Production of Hydrogen Peroxide from Water and Dioxygen with Bismuth Vanadate and a Cobalt(II) Chlorin Complex *ACS Energy Lett.*, **1**, 913-919 (2016).
229. Hong, A. P., Bahnemann, D. W. and Hoffmann, M. R., Cobalt(II) Tetrasulfophthalocyanine on Titanium Dioxide: A New Efficient Electron Relay for the Photocatalytic Formation and Depletion of Hydrogen Peroxide in Aqueous Suspensions *J. Phys. Chem.*, **91**, 2109-2117 (1987).
230. Harbour, J. R., Tromp, J. and Hair, M. L., Photogeneration of Hydrogen Peroxide in Aqueous Tio_2 Dispersions *Can. J. Chem.*, **63**, 204-208 (1985).
231. Cai, R., Hashimoto, K., Fujishima, A. and Kubota, Y., Conversion of Photogenerated Superoxide Anion into Hydrogen Peroxide in TiO_2 Suspension System *J. Electroanal. Chem.*, **326**, 345-350 (1992).
232. Assumpção, M. H. M. T., *et al.*, Comparative Study of Different Methods for the Preparation of Co_xo_y/C for the Electrosynthesis of Hydrogen Peroxide *Int. J. Electrochem. Sci.*, **6**, 1586-1596 (2011).
233. Cui, L., Ding, P., Zhou, M. and Jing, W., Energy Efficiency Improvement on in Situ Generating H_2O_2 in a Double-Compartment Ceramic Membrane Flow Reactor Using Cerium Oxide Modified Graphite Felt Cathode *Chem. Eng. J.*, **330**, 1316-1325 (2017).
234. Xu, F., *et al.*, A New Cathode Using CeO_2/MWNT for Hydrogen Peroxide Synthesis through a Fuel Cell *J. Rare Earth.*, **27**, 128-133 (2009).
235. Assumpção, M. H. M. T., *et al.*, Low Content Cerium Oxide Nanoparticles on Carbon for Hydrogen Peroxide Electrosynthesis *Appl. Catal., A*, **411-412**, 1-6 (2012).
236. Carneiro, J. F., Rocha, R. S., Hammer, P., Bertazzoli, R. and Lanza, M. R. V., Hydrogen Peroxide Electrogeneration in Gas Diffusion Electrode Nanostructured with Ta_2O_5 *Appl. Catal., A*, **517**, 161-167 (2016).
237. Carneiro, J. F., Paulo, M. J., Siaj, M., Tavares, A. C. and Lanza, M. R. V., Nb_2O_5 Nanoparticles Supported on Reduced Graphene Oxide Sheets as Electrocatalyst for the H_2O_2 Electrogeneration *J. Catal.*, **332**, 51-61 (2015).
238. Moraes, A., *et al.*, Use of a Vanadium Nanostructured Material for Hydrogen Peroxide Electrogeneration *J. Electroanal. Chem.*, **719**, 127-132 (2014).
239. Li, M. F., Liao, L. W., Yuan, D. F., Mei, D. and Chen, Y.-X., pH Effect on Oxygen Reduction Reaction at Pt(111) Electrode *Electrochim. Acta*, **110**, 780-789 (2013).
240. Marković, N. M. and Ross, P. N., Surface Science Studies of Model Fuel Cell Electrocatalysts *Surf. Sci. Rep.*, **45**, 117-229 (2002).
241. Duke, F. R. and Haas, T. W., The Homogeneous Base-Catalyzed Decomposition

of Hydrogen Peroxide *J. Phys. Chem.*, **65**, 304-306 (1961).
242. Kolyagin, G. A. and Kornienko, V. L., Kinetics of Hydrogen Peroxide Accumulation in Electrosynthesis from Oxygen in Gas-Diffusion Electrode in Acidic and Alkaline Solutions *Russ. J. Appl. Chem.*, **76**, 1070-1075 (2003).
243. Jebaraj, A. J. J., Georgescu, N. S. and Scherson, D. A., Oxygen and Hydrogen Peroxide Reduction on Polycrystalline Platinum in Acid Electrolytes: Effects of Bromide Adsorption *J. Phys. Chem. C*, **120**, 16090-16099 (2016).
244. Katsounaros, I., *et al.*, The Impact of Spectator Species on the Interaction of H_2O_2 with Platinum - Implications for the Oxygen Reduction Reaction Pathways *Phys. Chem. Chem. Phys.*, **15**, 8058-8068 (2013).
245. Shinozaki, K., Zack, J. W., Richards, R. M., Pivovar, B. S. and Kocha, S. S., Oxygen Reduction Reaction Measurements on Platinum Electrocatalysts Utilizing Rotating Disk Electrode Technique: I. Impact of Impurities, Measurement Protocols and Applied Corrections *J. Electrochem. Soc.*, **162**, F1144-F1158 (2015).
246. Yano, H., Uematsu, T., Omura, J., Watanabe, M. and Uchida, H., Effect of Adsorption of Sulfate Anions on the Activities for Oxygen Reduction Reaction on Nafion®-Coated Pt/Carbon Black Catalysts at Practical Temperatures *J. Electroanal. Chem.*, **747**, 91-96 (2015).
247. Ciapina, E. G., *et al.*, Surface Spectators and Their Role in Relationships between Activity and Selectivity of the Oxygen Reduction Reaction in Acid Environments *Electrochem. Commun.*, **60**, 30-33 (2015).
248. Mo, Y. and Scherson, D. A., Platinum-Based Electrocatalysts for Generation of Hydrogen Peroxide in Aqueous Acidic Electrolytes: Rotating Ring-Disk Studies *J. Electrochem. Soc.*, **150**, E39-E46 (2003).
249. Choi, C. H., *et al.*, Hydrogen Peroxide Synthesis Via Enhanced Two-Electron Oxygen Reduction Pathway on Carbon-Coated Pt Surface *J. Phys. Chem. C*, **118**, 30063-30070 (2014).
250. Kolyagin, G. A. and Kornienko, V. L., Effect of Trialkylammonium Salts and Current Density on the Electrosynthesis of Hydrogen Peroxide from Oxygen in a Gas-Diffusion Electrode in Acid Solutions *Russ. J. Appl. Chem.*, **79**, 746-751 (2006).
251. Stucki, S., Kötz, R., Carcer, B. and Suter, W., Electrochemical Waste Water Treatment Using High Overvoltage Anodes Part II: Anode Performance and Applications *J. Appl. Electrochem.*, **21**, 99-104 (1991).
252. Puértolas, B., Hill, A. K., García, T., Solsona, B. and Torrente-Murciano, L., In-Situ Synthesis of Hydrogen Peroxide in Tandem with Selective Oxidation Reactions: A Mini-Review *Catal. Today*, **248**, 115-127 (2015).
253. von Sonntag, C., Advanced Oxidation Processes: Mechanistic Aspects *Water Sci. Technol.*, **58**, 1015-1021 (2008).
254. Oh, D., Zhou, L., Chang, D. and Lee, W., A Novel Hydrogen Peroxide Stabilizer in Descaling Process of Metal Surface *Chem. Eng. J.*, **334**, 1169-1175 (2018).
255. Croft, S., Gilbert, B. C., Smith, J. R. L., Stell, J. K. and Sanderson, W. R., Mechanisms of Peroxide Stabilization. An Investigation of Some Reactions of Hydrogen Peroxide in the Presence of Aminophosphonic Acids *J. Chem. Soc., Perk. Trans. 2*, **2**, 153-160 (1992).
256. Watts, R. J., Finn, D. D., Cutler, L. M., Schmidt, J. T. and Teel, A. L., Enhanced Stability of Hydrogen Peroxide in the Presence of Subsurface Solids *J. Contam. Hydrol.*, **91**, 312-326 (2007).
257. Schumb, W., Stabilization of Concentrated Solutions of Hydrogen Peroxide *Ind. Eng. Chem.*, **49**, 1759-1762 (1957).
258. Harber, F. and Weiss, J., The Catalytic Decomposition of Hydrogen Peroxide by Iron Salts *Proc. R. Soc. London, Ser. A*, **147**, 332-351 (1934).
259. Davies, D. M., Dunn, D., Haydarali, M., Jones, R. M. and Lawther, J. M., The Formation and Radical Scavenging Properties of Ethylenediaminetetra-Acetic Acid *N*,*N*′-Dioxide in Aqueous *M*-Chloroperbenzoic Acid *J. Chem. Soc., Chem. Commun.*, **13**, 987-987 (1986).
260. Davies, D. M. and Jones, R. M., Kinetics and Mechanism of the Oxidation of Some Chelating Agents by Perbenzoic Acids *J. Chem. Soc., Perk. Trans. 2*, 1323-1326 (1989).
261. Baxendale, J. H. and Wilson, J. A., The Photolysis of Hydrogen Peroxide at High Light Intensities *Trans. Faraday Soc.*, **53**, 344-356 (1957).
262. Titova, K. V., Nikol'skaya, V. P., Buyanov, V. V. and Suprun, I. P., A Study of Stability of Potassium Fluoride Peroxosolvates $KF \cdot nH_2O_2$ (n = 1, 2) in Solid State and in Aqueous Solutions *Russ. J. Appl. Chem.*, **74**, 907-911 (2001).
263. Kolyagin, G. A. and Kornienko, V. L., Electrosynthesis of Hydrogen Peroxide in Solutions of Salts That Form Molecular Addition Products (Peroxo Solvates) with It *Russ. J. Electrochem.*, **50**, 798-803 (2014).
264. Cravotto, G., Carlo, S. D., Ondruschka, B., Tumiatti, V. and Roggero, C. M., Decontamination of Soil Containing Pops by the Combined Action of Solid Fenton-Like Reagents and Microwaves *Chemosphere*, **69**, 1326-1329 (2007).
265. Luo, H., Li, C., Wu, C. and Dong, X., In Situ Electrosynthesis of Hydrogen Peroxide with an

Improved Gas Diffusion Cathode by Rolling Carbon Black and PTFE *RSC Adv.*, **5**, 65227-65235 (2015).
266. Walsh, F. C. and Ponce de León, C., Progress in Electrochemical Flow Reactors for Laboratory and Pilot Scale Processing *Electrochim. Acta*, **280**, 121-148 (2018).
267. González-García, J., Banks, C. E., Šljukić, B. and Compton, R. G., Electrosynthesis of Hydrogen Peroxide Via the Reduction of Oxygen Assisted by Power Ultrasound *Ultrason. Sonochem.*, **14**, 405-412 (2007).
268. Oloman, C. and Watkinson, A. P., Hydrogen Peroxide Production in Trickle-Bed Electrochemical Reactors *J. Appl. Electrochem.*, **9**, 117-123 (1979).
269. Abdullah, G. H. and Xing, Y., Hydrogen Peroxide Generation in Divided-Cell Trickle Bed Electrochemical Reactor *Ind. Eng. Chem. Res.*, **56**, 11058-11064 (2017).
270. Foller, P. C. and Bombard, R. T., Processes for the Production of Mixtures of Caustic Soda and Hydrogen Peroxide Via the Reduction of Oxygen *J. Appl. Electrochem.*, **25**, 613-627 (1995).
271. Lei, Y., Liu, H., Jiang, C., Shen, Z. and Wang, W., A Trickle Bed Electrochemical Reactor for Generation of Hydrogen Peroxide and Degradation of an Azo Dye in Water *J. Adv. Oxid. Technol.*, **18**, 47 (2015).
272. McIntyre, J. A. and Phillips, R. F.,Electrolytic Synthesis of Hydrogen Peroxide in a Trickle Bed Cell in *Proceedings of the Symposium on Electrochemical Process and Plant Design*, Alkire, R. C., Beck, T. R. and Varjian, R. D. Editors, p. 79-97, The Electrochemical Society, Pennington, NJ (1983).
273. Yamada, N., Yaguchi, T., Otsuka, H. and Sudoh, M., Development of Trickle-Bed Electrolyzer for on-Site Electrochemical Production of Hydrogen Peroxide *J. Electrochem. Soc.*, **146**, 2587-2591 (1999).
274. Jirkovský, J. S., Busch, M., Ahlberg, E., Panas, I. and Krtil, P., Switching on the Electrocatalytic Ethene Epoxidation on Nanocrystalline RuO_2 *J. Am. Chem. Soc.*, **133**, 5882-5892 (2011).
275. Walsh, F. C., *A First Course in Electrochemical Engineering*, Electrochemical Consultancy, Romsey, UK (1996).
276. Steckhan, E., *et al.*, Environmental Protection and Economization of Resources by Electroorganic and Electroenzymatic Syntheses *Chemosphere*, **43**, 63-73 (2001).
277. Babu, K. F., Sivasubramanian, R., Noel, M. and Kulandainathan, M. A., A Homogeneous Redox Catalytic Process for the Paired Synthesis of L-Cysteine and L-Cysteic Acid from L-Cystine *Electrochim. Acta*, **56**, 9797-9801 (2011).
278. Matthessen, R., Fransaer, J., Binnemans, K. and De Vos, D. E., Paired Electrosynthesis of Diacid and Diol Precursors Using Dienes and CO_2 as the Carbon Source *ChemElectroChem*, **2**, 73-76 (2015).
279. Tatapudi, P. and Fenton, J. M., Simultaneous Synthesis of Ozone and Hydrogen Peroxide in a Proton-Exchange-Membrane Electrochemical Reactor *J. Electrochem. Soc.*, **141**, 1174-1178 (1994).
280. Espinoza-Montero, P. J., Vasquez-Medrano, R., Ibanez, J. G. and Frontana-Uribe, B. A., Efficient Anodic Degradation of Phenol Paired to Improved Cathodic Production of H_2O_2 at BDD Electrodes *J. Electrochem. Soc.*, **160**, G3171-G3177 (2013).
281. Paddon, C. A., *et al.*, Towards Paired and Coupled Electrode Reactions for Clean Organic Microreactor Electrosyntheses *J. Appl. Electrochem.*, **36**, 617 (2006).
282. Ito, S., Katayama, R., Kunai, A. and Sasaki, K., A Novel Paired Electrosynthesis of *p*-Benzoquinone and Hydroquinone from Benzene *Tetrahedron Lett.*, **30**, 205-206 (1989).
283. Ri-Yao, C., Zhen-Xia, H., Xi, Z. and Zhen, C., Paired Electro-Generation of Glyoxylic Acid Using Bipolar Membrane Made from Sodium Alginate and Chitosan *Chem. Eng. Commun.*, **197**, 1476-1484 (2010).
284. Bisselink, R. J. M. and van Erkel, J. Electrochemical Production of Hydrogen Peroxide. Europe Patent WO 2015/034354 A1 (2015)
285. Chhim, N., *et al*. Gas Diffusion Electrode, Apparatus and Process for the Production of Hydrogen Peroxide. EP 1 568 801 A1 (2005)
286. Nakajima, Y., Nishiki, Y., Uno, M., Katsumoto, A. and Nishimura, K. Process for the Production of Hydrogen Peroxide Solution. United States Patent US 2002/0130048A1 (2004)
287. Buschmann, W. E. and James, P. I. Methods and Apparatus for the On-Site Production of Hydrogen Peroxide. United States Patent US 2007/0074975 A1 (2010)
288. Mathur, I., James, A. and Bissett, D. Bipolar Electrolyzer. United States Patent 4927509 (1990)
289. Nakajima, Y., *et al.* Electrolytic Cell and Process for the Production of Hydrogen Peroxide Solution and Hypochlorous Acid. United States Patent US 6,773,575 B2 (2004)
290. Uno, M., Wakita, S., Sekimoto, M., Furuta, T. and Nishiki, Y. Electrolytic Cell for Hydrogen Peroxide Production and Process for Producing Hydrogen Peroxide. United States Patent US 6,767,447 B2 (2004)
291. Grigoropoulou, G., Clark, J. H. and Elings, J. A., Recent Developments on the Epoxidation of Alkenes Using Hydrogen Peroxide as an Oxidant *Green Chemistry*, **5**, 1-7 (2003).
292. Ibanez, J. G., Frontana-Uribe, B. A. and Vasquez-Medrano, R., Paired Electrochemical

Processes: Overview, Systematization, Selection Criteria, Design Strategies, and Projection *J. Mex. Chem. Soc.*, **60**, 247-260 (2016).
293. Pletcher, D., The Cathodic Reduction of Carbon Dioxide—What Can It Realistically Achieve? A Mini Review *Electrochem. Commun.*, **61**, 97-101 (2015).
294. Wu, J. and Zhou, X.-D., Catalytic Conversion of CO_2 to Value Added Fuels: Current Status, Challenges, and Future Directions *Chin. J. Catal.*, **37**, 999-1015 (2016).
295. Lu, H.-F., Chen, H.-F., Kao, C.-L., Chao, I. and Chen, H.-Y., A Computational Study of the Fenton Reaction in Different Ph Ranges *Phys. Chem. Chem. Phys.*, **20**, 22890-22901 (2018).
296. Kremer, M. L., The Fenton Reaction. Dependence of the Rate on Ph *The Journal of Physical Chemistry A*, **107**, 1734-1741 (2003).
297. Castañeda, L. F., Walsh, F. C., Nava, J. L. and Ponce de León, C., Graphite Felt as a Versatile Electrode Material: Properties, Reaction Environment, Performance and Applications *Electrochim. Acta*, **258**, 1115-1139 (2017).
298. Walsh, F. C., Arenas, L. F. and Ponce de León, C., Developments in Electrode Design: Structure, Decoration and Applications of Electrodes for Electrochemical Technology *Journal of Chemical Technology & Biotechnology*, **93**, 3073-3090 (2018).
299. Walsh, F. C., *et al.*, The Continued Development of Reticulated Vitreous Carbon as a Versatile Electrode Material: Structure, Properties and Applications *Electrochim. Acta*, **215**, 566-591 (2016).